




A possible 5 km wide impact structure with associated 22 km wide exterior collapse terrain in the Alhabia–Tabernas Basin, southeastern Spain

Sebastián Tomás SÁNCHEZ GÓMEZ¹, Jens ORMÖ ², Carl ALWMARK ³,
 Sanna HOLM-ALWMARK³, Gabriel ZACHÉN³, Robert LILLJEQUIST⁴, and
 Juan Antonio SÁNCHEZ GARRIDO ^{1*}

¹Departamento de Agronomía, Universidad de Almería, Almería, Spain

²Centro de Astrobiología (CAB), INTA-CSIC, Instituto Nacional de Técnica Aeroespacial-Consejo Superior de Investigaciones Científicas, Carretera de Ajalvir km 4, Torrejón de Ardoz, Madrid, Spain

³Department of Geology, Lund University, Lund, Sweden

⁴Eurogeologist, Estepona, Málaga, Spain

*Correspondence

Juan Antonio Sánchez Garrido, Departamento de Agronomía, Universidad de Almería, Ctra Sacramento s/n. 04120, Almería, Spain.

Email: jasanche@ual.es

(Received 04 May 2022; revision accepted 31 July 2023)

Abstract—The Tabernas–Alhabia Basin is a structural depression situated in the province of Almería, southeastern Spain. The basin is filled with Neogene, Pliocene, and Pleistocene sediments resting discordantly on a Paleozoic metamorphic basement. During the marine Tortonian sedimentation, a bed of breccia (Gordo megabed) was formed. It consists of rotated sedimentary megablocks commonly capped and/or surrounded by a polymict breccia composed mainly of up to dm-sized clasts of the crystalline (schist) basement. Previous work has suggested the bed to be a seismite corresponding to events induced by earthquakes. Here, we link the formation of the Gordo megabed with an ~5 km wide, rimmed depression with exposed breccias on the northern flank of the Sierra de Gádor mountain. This semicircular structure, developed in mainly schists and dolostone of the basement, is delimited to the W, S, and E by an up to 350 m high escarpment with overturned stratigraphy. Toward the north, this crater-like structure opens toward the Gordo megabed of the Tabernas Basin. In the southern sector, the overturned strata transform outward for into a blocky allochthonous breccia with decreasing thickness and clast size. In the interior of the structure, there are occurrences of graded breccia and arenite superposed on a blocky, autochthonous breccia. Based on the presence of mineralogical shock metamorphic evidence, potential shatter cones, and a high Ir anomaly (~500 ppb) as well as the position of the structure near the town of Alhama de Almería, we propose to call it the Alhama de Almería impact structure.

INTRODUCTION

Background and Aim of Study

For a long time, many of the now confirmed terrestrial impact structures were considered as a result of ordinary geologic processes, for example, volcanism, tectonic movements, erosion. However, later detailed studies of rocks from these structures showed that they

had been subject to high-pressure transformations, or inclusion of elements, not normally occurring on the surface of the Earth, which may only be due to high-velocity collisions with cosmic bodies. The investigation of surfaces of solid planets and various asteroids showed that impact cratering plays a fundamental role in the solar system (Melosh, 1989; Osinski & Ferrière, 2016; Osinski & Pierazzo, 2012). A little over 200 terrestrial impact structures have been confirmed to date (Osinski

et al., 2022), their number increasing every year, not only due to new discoveries in geologically poorly studied areas but also as a result of the use of new diagnostic methods in previously well-studied regions (Masaitis & Naumov, 2020).

The aim of this study is the description and reinterpretation of the geology, sedimentary structures, and geomorphological features in parts of the Tabernas Basin and Sierra de Gádor that could be related to a cosmic impact and to suggest a possible candidate site for this impact.

For some observed geological and geomorphological features, we here apply the terminology used for comparable impact-related structures. This is to facilitate a direct comparison in context with the impact cratering process.

Geographical and Geological Setting

The sedimentary Neogene basins in the province of Almería in southeastern Spain include:

- a. Alhabia Basin trending E–W, limited to the north by the Sierra de Filabres and Sierra Nevada and to the south by Sierra de Gádor.
- b. Tabernas Basin, a northeast prolongation of the Alhabia Basin, located between Sierra de Filabres, Sierra Alhamilla, and Sierra de Gádor.
- c. Gádor-Almería Basin, oriented NW–SE.

These basins formed during Miocene by a substantial subsidence on the order of 1200 m (Cloetingh et al., 1992) and are filled with Neogene, Pliocene, and Pleistocene sediments, which are discordantly deposited on a Paleozoic metamorphic basement (Figure 1).

The basins are located in the Internal Zone of the Betic Cordillera and are structurally configured as elongated intramontane basins in a collisional orogen (Martínez Martos et al., 2017). The basement in which the basins developed is made up of metamorphic rocks, which today are exposed in the mountains limiting the basins. The basins are filled unconformably by post-orogenic detrital materials from Serravallian until Quaternary (Dabrio et al., 1981, 1985; Serrano, 1990).

The mountains limiting the basins consist of two complexes of the Betic Cordillera that emerge in southern Spain. They have been subject to high-pressure Alpine metamorphism (chloritoid-rich graphite schist and quartzites) beginning during the Serravallian (13.6–11.6 Ma; Martínez & Azañón, 2002). The Nevado-Filábride metamorphic complex (NFC) appears in the interiors of the Sierra de Filabres, Sierra Nevada, and Sierra Alhamilla (Jong & Bakker, 1991). The Alpujárride Complex (AC; Akkerman et al., 1980) appears in the Sierra de Gádor and Sierra Alhamilla (Figure 1). The NFC is generally subdivided into a lower unit, consisting of a

lithologically monotonous sequence of Middle Devonian graphite–micaschists and quartzites (Gómez Pugnaire et al., 2012). The AC consists of a Middle to Upper Triassic carbonate formation, as well as fine-grained, light-colored schists and gray phyllites, generally thought to be Permian–Triassic (Akkerman et al., 1980).

The Neogene sediments in the area are commonly referred to as deep water marls corresponding to a slope facies (Weijermars, 1991; Figure 2). The lithology consists of alternating sands, sandstones, and silty marls interspersed with breccia occurrences resting unconformably on the basement (Martín & Braga, 2001).

Paleogeographically, from late Tortonian, the Neogene basins are surrounded by the Paleozoic basement high reliefs of Sierra de Filabres, Sierra Nevada, Sierra de Gádor, and Sierra Alhamilla (Weijermars et al., 1985). These basins are suggested to have formed an up to 400–600 m deep sea bay (Poisson et al., 1999), with a very shallow continental shelf that connected to the continental slope with a set of turbidite systems and submarine fans (Kleverlaan, 1989b, 1989c). The relative chronology established by the planktonic foraminifera, calcareous nannoplankton, and microfauna establishes the age of these turbidite sediments at about 8 Ma, late Tortonian (Berggren et al., 1995).

The end of Tortonian coincided with a compressive tectonic event in NNW–SSE to N–S direction, which affected both the basement and Neogene deposits hosted in the basins (García Tortosa & Sanz de Galdeano, 2007; Sanz de Galdeano et al., 2006). This resulted in the uplift of the basement and a strong dip of Neogene sediments in contact with it (Martínez & Azañón, 2002). A subsequent isostatic adjustment during the Pliocene led to further general uplift of the region (Cloetingh et al., 1992; Kleverlaan, 1987), causing erosion leading to sedimentation of conglomerates and sandstones in fluvial and alluvial fan systems (Harvey et al., 2003). These sediments spread into the surrounding areas and lie discordant on the metamorphic basement and older Neogene sediments (Martín Penela et al., 1997). Thus, this general emergence of the region resulted in a change from marine to continental deposition in the basins. Continued uplift during the Quaternary caused a transition to the net erosional conditions prevailing in the modern landscape (Harvey, 2001). This tectonic elevation has allowed the identification of the different Tortonian sedimentary structures which abound in both the Alhabia and Tabernas basins.

One of the most conspicuous sedimentary features of the Tabernas Basin, essential for our here presented impact scenario, is a tens of meters thick package of detrital sediment suggested to have been deposited in a marine setting (cf. Braga et al., 2003). Kleverlaan (1987) described these deposits in detail and grouped them into a unit called the Gordo megabed.

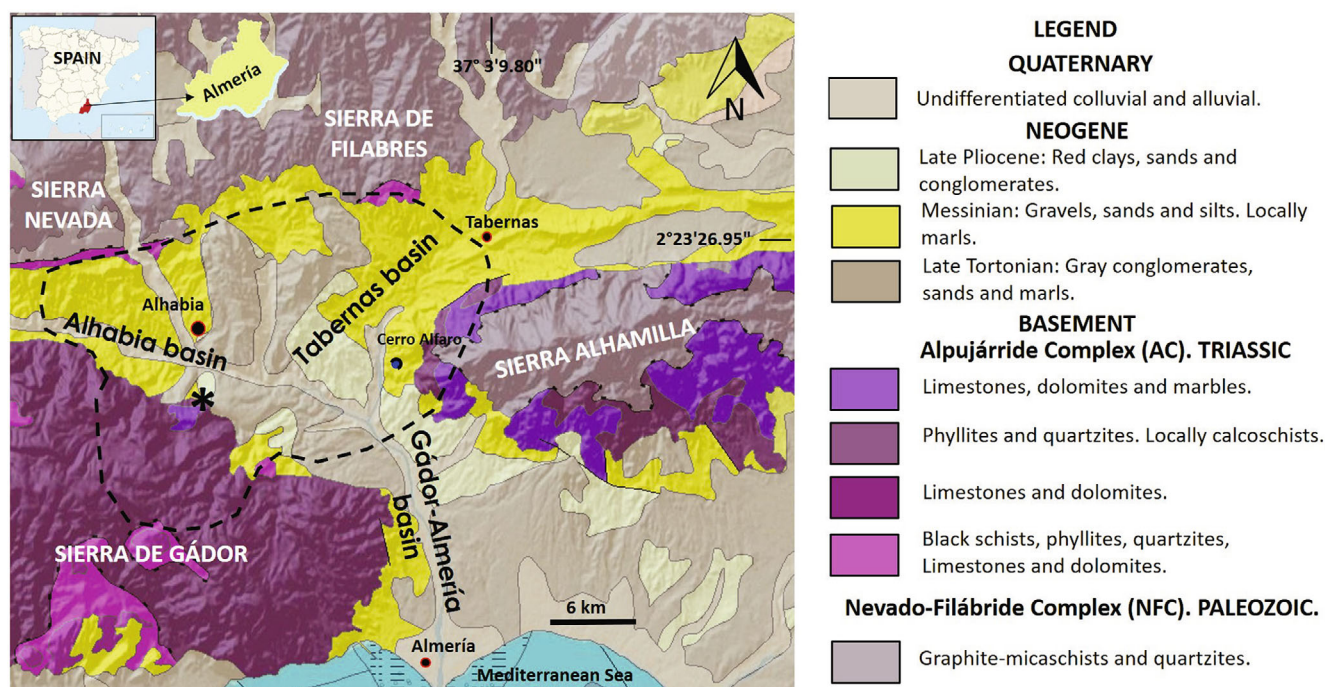


FIGURE 1. General geological setting of the Neogene basins: Alhabia Basin, Tabernas Basin, and Gádor-Almería Basin, situated in southeastern Spain in the province of Almería. (Data from Cartographic viewer with georeferenced topography, Instituto Geológico y Minero de España, IGME, 2023). A magnification of the inset is shown in Figures 3 and 9. Stippled line indicates the apparent maximum extent of the disturbed zone. Gordo megabed belongs to the late Tortonian.

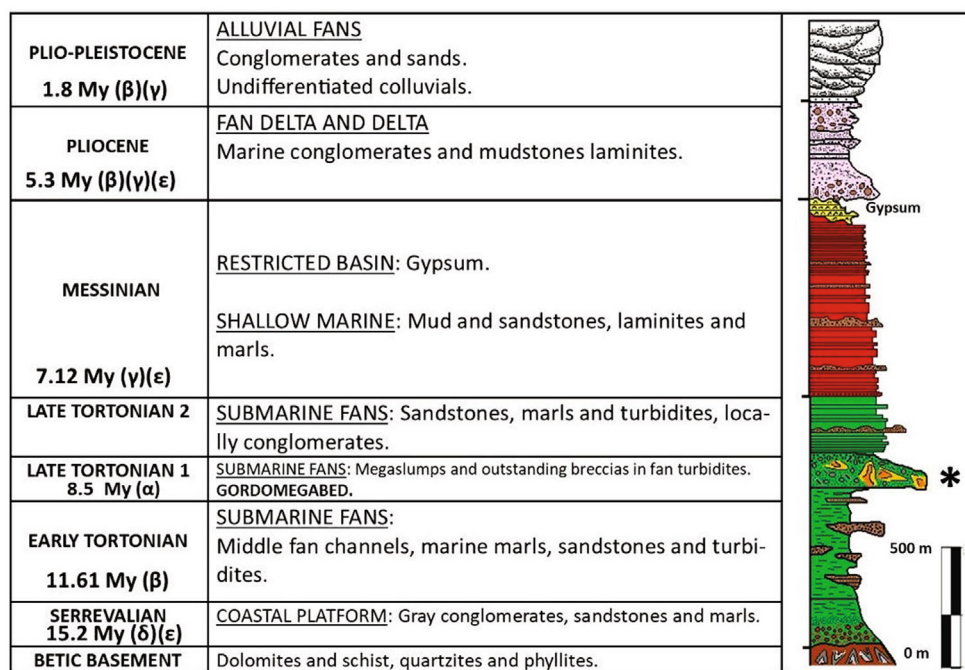


FIGURE 2. Stratigraphic succession of Neogene and Quaternary sediments of the Tabernas Basin (Modified from: [α] Berggren et al., 1995; [β] Crespo-Blanc et al., 2016; [γ] García-García et al., 2006; [δ] Sanz de Galdeano & Vera, 1991; and [ε] Weijermars, 1991). Star indicates the stratigraphic position of the proposed impact event and related lithologies.

The Gordo Megabed

The Gordo Megabed is an informal, 60–70 m thick, sedimentary rock unit, which is exposed in several outcrops in the Tabernas Basin (Braga et al., 2003; Kleverlaan, 1987). It is suggested to have formed during the late Tortonian in a slope setting with continuation out on the submarine plain at up to 400–600 m of depth (Braga et al., 2003). The Gordo megabed consists of two sedimentary units:

1. A large mega-slump unit consisting of deformed layers of sandstones and siltstones of a turbiditic facies.
2. A clast-supported breccia with clasts of graphite–micaschist, quartzite, and gneiss. Kleverlaan (1989a) interpreted the breccia as a seismite caused by collapse during the deposition of Upper Tortonian fan turbidites.

The Gordo megabed is exposed for 11.5 km in N–S direction and 17 km in E–W direction. The total volume of the megabed is conservatively estimated to 6 km³, considering an average (compacted) thickness of 30 m. The volume of extrabasinal (its origin is in the surrounding metamorphic reliefs) components is estimated at 0.9 km³ (Kleverlaan, 1987).

Alternatively, the Gordo megabed was suggested by Cronin (1994, 1995) and Haughton (2000) to be the result of an interaction of different turbidite systems, tectonic activity, and bathymetric changes, leading to syndepositional collapse breccias at the edge of the basin.

Other late Tortonian catastrophic events have been suggested to be recorded in the Gordo megabed, such as tsunamites described in the Rambla de Indalecio in Tabernas Basin and interpreted as the effect of an earthquake (Puga Bernabéu et al., 2007). The word “rambla” is used in this part of Spain for what geomorphologically is called a wadi, that is, a riverbed that contains water only in connection with heavy rain.

Area of Extensive Brecciation and Overturning of Strata at the Contact Between the Alhabia–Tabernas Basin and the Northern Slope of Sierra de Gádor: The Location of the Proposed Impact Structure

This approximately 6 km wide area is located next to the small town of Alhama de Almería. It forms a topographic depression on the northern slope of Sierra de Gádor just at the transition to the southwestern margin of the Alhabia–Tabernas Basin (Figure 1). Sierra de Gádor is a large antiform made up of Paleozoic to Triassic Betic basement rocks and trending E–W to ENE–WSW (Voermans, Baena, Martínez, et al., 1983). Previous studies of this area describe the so-called Felix

and Gádor nappes, that is, the stacking of tectonic units that form the north-eastern flank of Sierra de Gádor (Martín, 2006; Sanz de Galdeano, 1985; Sola et al., 2018; Voermans, Baena, Ewert, et al., 1983). The lithological succession in this area of the Alpujárride nappes (Felix and Gádor nappes) includes phyllites, quartzites, and gypsum, at the base, followed by carbonaceous schists and dolostones (in many cases as intraformational breccias), with minor limestones, altogether >600 m in thickness. All these rocks are Permian–Triassic in age (Voermans, Baena, Ewert, et al., 1983). In this area, Sola et al. (2018) describe a late Miocene (8.5–7.5 Ma), submarine landslide that forms a 5.6 km long and 5.2 km wide slump scar. The slump scar has a semicircular shape; at its foot, there are described coherent large masses of metamorphic rocks and Miocene breccias, marine bioclastic conglomerates, and sandstones, comprising clast from AC, that distally change to chaotic deposits of blocks of different lithologies. These are embedded in upper Tortonian marine marls and high-strength cohesive debris. The triggering mechanism of the so-called Alhama de Almería Slide is said to be seismic activity related to the tectonic instability of Sierra de Gádor during the late Tortonian. The NW–SE and WNW–ESE normal faults of variable scale related to this compression affect basement rocks and Neogene to Quaternary deposits (Marín-Lechado et al., 2007; Pedrera et al., 2012). Notably, this suggested tectonic instability is coeval with the seismites of varying dimensions in the adjacent Alhabia–Tabernas Basin, that is, the Gordo megabed. Likewise, the chaotic deposits described at the foot of the “slump scar” coincide with those of the local occurrence of the Gordo megabed. It is also important to take into account that the northern boundary of the “slump scar” is affected by the so-called Andarax fault zone, characterized by both normal and dextral strike-slip movement (Marín-Lechado et al., 2007; Martín, 2006; Martínez Martos et al., 2017; Pedrera et al., 2012). Likewise, at the S–SE rear end (escarpment) of the “slump scar” target material at the scale of tens of meters are described as vertically standing bedding (Martín, 2006) or even inverted (Sanz de Galdeano, 1985).

Together, these published observations as well as our own work suggest that this “slump scar” is the site of the impact that we propose to have affected the study area.

MATERIALS AND METHODS

Multiple field studies were carried out over the course of 17 years by the authors (S.T.S.G., J.O., R.L., and J.A.S.G.) to study the geology and geomorphology of the Tabernas Basin and its surroundings with special focus on the Gordo megabed. During the last year, after the

suspicions that the Gordo megablock could be impact-related had strengthened, the fieldwork came to include also the suspected impact site on the flank of Sierra de Gádor. These field studies were carried out with a combination of geological mapping and the measurement of parameters of the observed geological structures, both in situ (using GPS Garmin eTrex Legend) and georeferenced LIDAR topographic data (Ministerio de Transportes, Movilidad y Agenda Urbana, 2019) with resolution of 0.5 p m⁻². All the identified structures are shown in Figure 3. The reference codes of the structures are used henceforth in all the annexed tables.

Thin sections (410 in total) for petrographic studies and the search for shock metamorphic evidence were prepared, in the great majority of cases after extracting a residue of quartz grains by dissolving the material in 15% acetic acid. The search for shock metamorphic features a Nikon Eclipse LV100N POL optical microscope at the Research Central Services of Almería University and with an Olympus BX53 optical microscope at the Department of Geology of Lund University. Quartz grains displaying planar features were further studied using a Leitz 5-axes Universal Stage (Department of Geology, Lund University) and the orientations of optic axes (*c*-axis) and the poles perpendicular to planes in individual quartz grains were determined following the techniques described by von Engelhardt and Bertsch (1969), Stöfler and Langenhorst (1994), and Ferrière et al. (2009). The orientation of the optic axis and the poles perpendicular to planes were plotted by hand in a stereographic Wulff net and then indexed with Miller–Bravais indices (hkil), using the stereographic projection template of Ferrière et al. (2009).

At the Central Research Services of the University of Almería samples were also studied with a scanning electron microscope (SEM) Hitachi S-3500N, equipped with a secondary and backscattered electron detector, RX probe, and energy-dispersive spectrometer (EDS). Platinum group elements (PGEs) were analyzed in a mass spectrometer iCAP TQ ICP-MS (Thermo Fisher). Before analysis, the samples were prepared with a mixture of nitric, hydrochloric, and hydrofluoric acids in an UltraWAVE “ERC” (MILESTONE) until completely dissolved.

RESULTS

Field Observations

Megablocks

We define megablocks as coherent lithic blocks that are tilted or rotated, lithologically homogeneous (commonly set of turbidites), and that extend in outcrop over at least 30 meters (i.e., having dimensions of several

tens of meters; Table 1). Three zones of megablocks have been identified and mapped (Figure 3a–c):

- Zone 1: Central part of Tabernas Basin, especially at the Rambla de Tabernas (Figure 4a–d).
- Zone 2: Borders to Zone 1 to the east and the Cerro Alfaro hill (Figure 4e).
- Zone 3: Alhabia Basin (part of greater Tabernas Basin), adjacent to the “slump scar” at Alhama de Almería on the northern flanks of Sierra de Gádor (Figure 4f).

With the “ramblas” passing between the megablocks, the characteristic hummocky relief of the basins is created. The altitude of the high reliefs ranges between 270 and 744 m a.s.l., while their length varies from 73 to 1073 m. Their slopes vary considerably, from 20° to 50°. Although the megablocks present an irregular distribution pattern, there is in Megablock Zones 1 and 2 an overall tendency to dip toward the W (Figure 4a), and in Megablock Zone 3 toward the E, that is, in both instances in the direction of Alhama de Almería (i.e., the location of the proposed impact structure). However, this is not always the case as the alignment of some megablocks seems also affected by the structural direction of the basin. Several outcrops among the megablocks feature a polymict breccia consisting exclusively of clasts of Paleozoic basement (Figure 4b and background of Figure 4c) of Nevado-Filábride complex and occasionally brecciated dolomite (AC; foreground of Figure 4c).

Plastically Deformed Megablocks

Our field studies have revealed only three outcrops of what we here refer to as “Plastically Deformed Megablocks”; SB1, SB2, and SB3 (Figure 5). They involve recumbent folds with reverse limb whose fold axes follow the direction: N25E, N275E, and N210E (Table 1). They are located in Rambla Seca (SB1) and Rambla de Tabernas (SB2 and SB3), respectively. They appear at the lowest altitudes of all the mapped structures in the area, that is, at 217, 207, and 290 m a.s.l. They are located within the Tabernas Basin rather than on its edges. They express strong plastic internal deformation of the, within the slump unit, mobilized stacks of late Tortonian turbiditic marl and sandstones beds. The deformed blocks are generally inclined to the NE, W, and SW (Table 1). The direction of the fold axes of the plastically deformed megablocks does not match the main tectonic directions of the Neogene basins, that is, E–W to NE–SW (Martínez Martos et al., 2017).

The plastically deformed megablocks express internal ductile deformation and are embedded among different, merely tilted blocks (Figure 5). On top of, but in some instances also wedged in between the tilted blocks, there

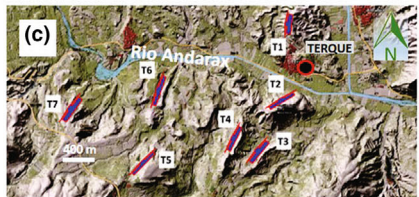
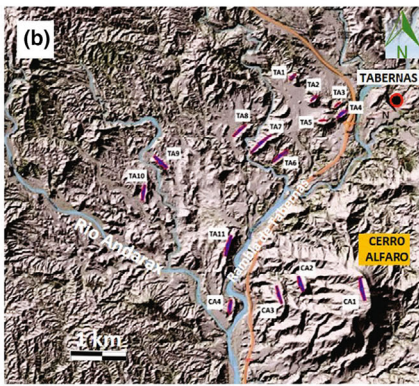
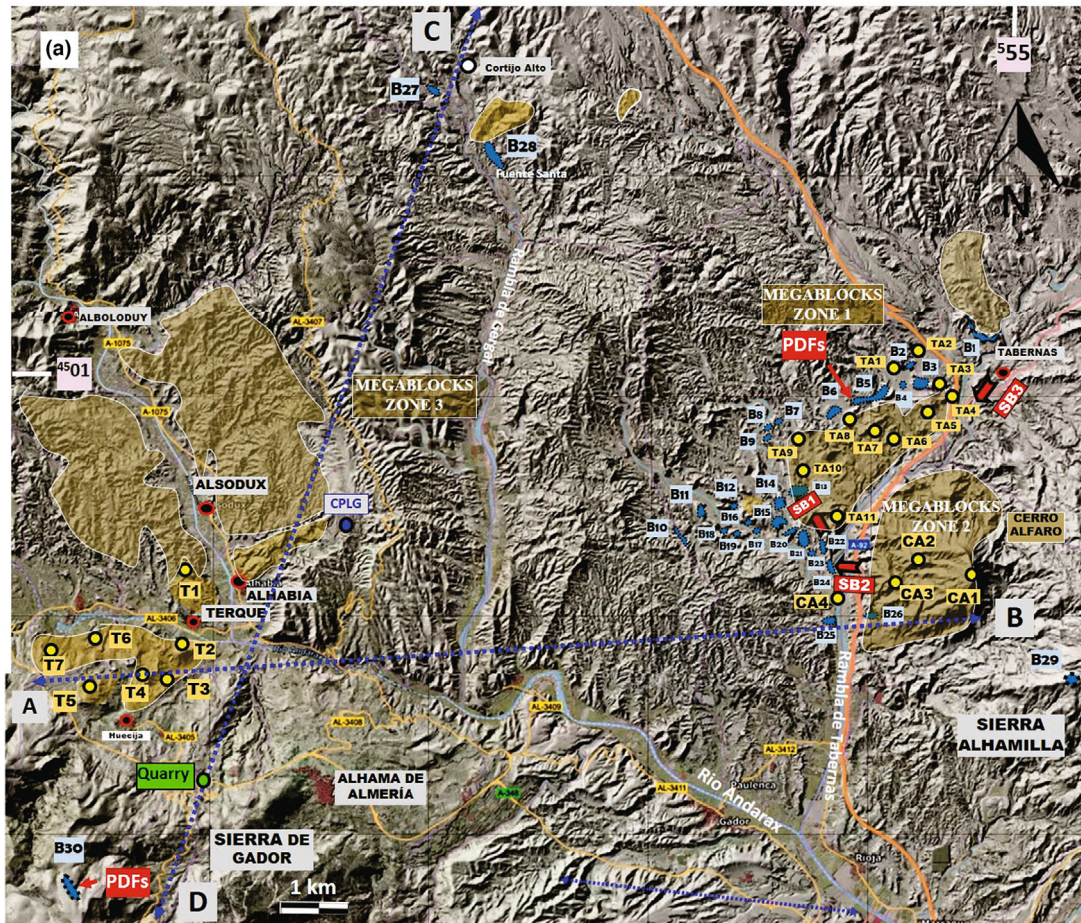


FIGURE 3. Distribution of putatively impact-related features and lithologies within the Tabernas Basin (i.e., exterior impact-affected terrain). (a) General location and distribution of the structures overlaid on a georeferenced LIDAR image, viewer iberpix4 (Instituto Geográfico Nacional, IGN, 2023). The cross sections A–B and C–D (conceptual scheme cross sections) are shown in Figure 13. The “quarry” indicates location of possible shatter cones (see Figure 10) and the suggested center of the crater (Figure 13). (b) Georeferenced cartography in LIDAR image of megablocks in Zone 1 (Rambla de Tabernas) and Zone 2 (Cerro Alfaro). (c) Georeferenced cartography in LIDAR image of megablocks in Zone 3 (Terque). (d) Extension, location, and distribution of the exposed polymict breccias in Tabernas basin, LIDAR map. Location of samples analyzed for shock evidence, PDFs. Abbreviations used: *B*: Breccia (*B1* and *B2*: Figure 4d; *B4*: Figure 6a; *B5*: Figures 4b, 6b,c,d; *B10*: Figure 4c; *B29*: Figures 6e,f and 7a,b; *B30*: Figure 6g). Megablock position: *TA*: Tabernas (*TA1* and *TA2*: Figure 4d; *TA3*: Figure 4a; *TA 8*: Figure 4b). *CA*: Cerro Alfaro (*CA1*: Figure 4e). *T*: Terque (*T1*, *T2*, *T3*, *T4* and *T6*: Figure 4f). *SB*: Plastically deformed megablocks (*SB1*: Figure 5a; *SB2*: Figure 5b; *SB3*: Figure 5c). Note how the course of the ramblas runs among the megablocks. “Rambla” is the local name for the geographical term wadi, an ephemeral riverbed.

is a polymict breccia consisting of graphite–micaschist, quartzite, and gneiss (Nevado-Filábride Complex), as well as dolomite (AC) appears. It commonly occurs as erosional remnants of an originally more extensive bed (Figure 4c).

Outcrop SB3 (location Figure 3a, appearance Figure 5c) is a typical example of the Gordo megabed (Kleverlaan, 1987) consisting of two sedimentary units:

1. A large megablock showing a single, low-angle fold of deformed layers of sandstones and silts of turbiditic facies.
2. A clast-supported polymict breccia of graphite–micaschist, quartzite, and gneiss, previously interpreted as a seismite developed in material belonging to Upper Tortonian fan turbidites.

The totality of this megablock slump does not emerge on the surface. The parts visible today have been preserved by sedimentation at the end of the Tortonian and later become exposed by the fluvial erosion forming the Rambla de Tabernas. The contact between the two units is apparent through the erosional surface at the top of the slump unit. This would, in the model that we propose, correspond to an earlier, albeit denudated, topography of the structure (Figure 5c).

Polymict Breccias

Table 1 presents the main characteristics of the numerous breccias identified in the Tabernas Basin and the surrounding mountain ranges.

Polymict breccias (localities B1–B28, Figure 3a,b) are commonly located at the Rambla de Tabernas, at an altitude of 204–324 m a.s.l., although a small proportion are to be found also to the north of the Rambla de Gérgal in Cortijo Alto at altitudes of 511–568 m a.s.l. (Figure 3d). Likewise, polymict breccias (B29 and B30) are also occurring at higher altitudes (820 and 1138 m a.s.l.) in Sierra Alhamilla and Sierra de Gádor (Figure 3a).

The breccias B1–B28 form a single lithostratigraphic unit that includes material from NFC (mainly graphite–micaschist, quartzite, and gneiss), as well as brecciated

dolomite of AC. Stratigraphically and geographically, these breccias occur at the area of the Alhama de Almería “slump scar” or as incorporated in the megablock slump deposits in the central parts of the Tabernas Basin (Figure 4b,c). The Tabernas Basin localities do not occur along the flanks of the basin as would be expected if formed by scree from the mountain ranges. Likewise, are not associated with any visible or known fault system, which is further excluded by their geographical distribution and stratigraphic position.

For most parts, the polymict breccias related to the Gordo megabed within the Tabernas Basin are heavily eroded with mainly coarse clastics forming an erosional residue having lost much of the fine matrix material in the exposed parts. The material often has a dark color due to dominant lithological composition, graphite–micaschist. As a result, most of these erosional remnants appear as poorly consolidated debris covering an often rotated megablock resulting in a dark, conical landforms that we choose to call *Black Hills* (Figure 6a).

Typical examples of this breccia occur at localities B4 (Figures 3 and 6a) and B5 (Figures 3 and 6b,c). They are massive, unstratified, clast supported and lack visible sedimentary structures. Weathered rims on clasts are absent. The angular shape of the fragments would indicate short transport, but the basement clast lithologies of the breccia originate far from the present locations. The clasts bear no signs of preferential direction of flow, for example, imbrication. In addition, quartzite clasts in breccia B5 commonly show marked fractures, mostly open, parallel, or subparallel to each other (Figure 6d).

Breccia B29 is in an anomalous stratigraphic position on Triassic phyllites of the AC (Figures 6e,f and 7a,b). The breccia constitutes a variable 10–50 cm thick deposit of Neogene material (loams and sometimes sands and limestones) and covering a surface of approximately 450 m². The loamy material is massive, unconsolidated, and its texture is highly uniform, with 95% of its particles of less than 50 μm (Figure 7c).

In the fraction of particles between 50 and 250 μm, the presence of a Neogene assemblage of planktonic and

TABLE 1. General characteristics of megablock zones and plastically deformed megablocks and polymict breccias.

Ref	Coordinates (UTM)	Elevation (m)	Outcrop length (m)	Character	Orientation/DIP
Megablock Zone 1 (Rambla Tabernas)					
TA1*	30SWF4853297965	350	383	LT	N40E/50NW
TA2*	30SWF4883697464	347	85	LT	N50E/45 NW
TA3*	30SWF4918297359	297	126	LT	N50E/45 NW
TA4	30SWF4925997176	313	73	LT	N50E/45 NW
TA5	30SWF4906597077	326	177	LT	N80E/45 N
TA6	30SWF4827696481	270	207	LT	N53E/15NW
TA7	30SWF4795196695	296	321	LT	N50E/45 NW
TA8*	30SWF4754596813	298	166	LT	N45E/45 NW
TA9	30SWF4618396305	307	234	LT	N100E/40SW
TA10	30SWF4594795840	303	261	LT	N10E/55 W
TA11	30SWF4732894940	304	462	LT	N15E/25 W
Megablock Zone 2 (Cerro Alfaro)					
CA1*	30SWF4976294275	744	1073	LT	N170E/35 W
CA2	30SWF4868594381	419	304	LT	N165E/30 W
CA3	30SWF4830494096	351	465	LT	N165E/35 W
CA4	30SWF4747094018	242	95	LT	N10E/30 W
Megablock zone 3 (Terque)					
T1*	30SWF3583193670	369	453	LT	N10E/20E
T2*	30SWF3579392670	413	425	LT	N70E/35SE
T3*	30SWF3555292106	370	568	LT	N47E/25SE
T4*	30SWF3515092105	395	670	LT	N20E/40E
T5	30SWF3413891836	501	250	LT	N40E/30SE
T6*	30SWF3433592950	332	439	LT	N21E/20E
T7	30SWF3319892559	437	183	LT	N42E/20SE
Ref	Coordinates (UTM)	Elevation (m)	Outcrop length (m)	Character	Direction fold axis/Vergence
Plastically deformed megablocks (Age: Late Tortonian)					
SB1*	30SWF4687994529	217	40	Turbidity system	N25E/NE
SB2*	30SWF4737694114	207	120	Turbidity system	N275E/W
SB3*	30SWF5208640993	290	77	Turbidity system	N210E/SW
Ref	Coordinates (UTM)	Elevation (m)	Outcrop length (m)	Character	
Polymict Breccia (Age: Late Tortonian)					
Tabernas Rambla					
B1*	30SWF4994998378	324	77	Poorly consolidated (BH)	
B2*	30SWF4866197681	301	20	Poorly consolidated (BH)	
B3	30SWF4875597498	317	120	Poorly consolidated (BH)	
B4*	30SWF4855597436	286	65	Poorly consolidated (BH)	
B5*	30SWF4801797203	263	563	Consolidated	
B6	30SWF4729596979	302	130	Consolidated	
B7	30SWF4632496755	317	57	Poorly consolidated (BH)	
B8	30SWF4622796646	306	90	Poorly consolidated (BH)	
B9	30SWF4608996546	291	65	Poorly consolidated (BH)	
B10*	30SWF4452594883	280	310	Poorly consolidated (BH)	
B11	30SWF4495095135	306	150	Poorly consolidated (BH)	
B12	30SWF4553795196	258	78	Poorly consolidated (BH)	
B13	30SWF4661595481	309	210	Poorly consolidated (BH)	
B14	30SWF4629595385	280	330	Poorly consolidated (BH)	
B15	30SWF4609995013	291	330	Consolidated	
B16	30SWF4579494933	237	50	Poorly consolidated (BH)	
B17	30SWF4589594853	236	87	Poorly consolidated (BH)	
B18	30SWF4546494919	250	98	Poorly consolidated (BH)	

TABLE 1. *Continued.* General characteristics of megablock zones and plastically deformed megablocks and polymict breccias.

Ref	Coordinates (UTM)	Elevation (m)	Outcrop length (m)	Character
B19	30SWF4547194783	255	60	Poorly consolidated (BH)
B20	30SWF4643794798	241	117	Poorly consolidated (BH)
B21	30SWF4678394746	286	200	Poorly consolidated (BH)
B22	30SWF4712894539	246	232	Poorly consolidated (BH)
B23	30SWF4685994522	214	56	Poorly consolidated (BH)
B24	30SWF4723494141	204	166	Poorly consolidated (BH)
B25	30SWF4762793297	198	76	Poorly consolidated (BH)
B26	30SWF4792193313	206	56	Poorly consolidated (BH)
Gergal Rambla				
B27	30SWG3995802821	568	276	Consolidated
B28	30SWG4103901628	511	605	Poorly consolidated (BH)
Sierra Alhamilla				
B29*	30SWF5183992211	820	45	Unconsolidated Neogene
Sierra De Gador				
B30*	30SWF5335088570	1138	10	Mix Triassic basement and Neogene
B31*	30SWF5331540883	1103	30	Triassic basement consolidated
B32*	30SWF5346440843	987	51	Triassic basement consolidated
B33*	30SWF8383540881	585	100	Triassic basement consolidated
B34*	30SWF8383740881	584	75	Triassic basement consolidated
B35*	30SWF5360640899	646	80	Triassic basement consolidated
B36*	30SWF5381740879	522	15	Triassic basement consolidated
B37*	30SWF5375940871	700	300	Mix Triassic Basement and Neogene
B38*	30SWF5374440868	737	500	Mix Triassic Basement and Neogene

Note: Lithology: Sandstones, marls, and breccias. Lithology breccias 1–28: graphite–micaschists and quartzites. Breccia 29: mix marls and sandstones. Breccia 30: mix marls, sandstones, dolostones, and phyllites. *Field observations with photo. General location, distribution, and more detail at the bottom of Figures 3 and 9. From each sample, a thin section has been made (in total 410 thin sections). B35*: Quarry Cirera Humberón S.L. Sample 1: B5. Sample 2: B29. Sample 3: B30. Sample 4: 30SWF3977687137.

Abbreviations: CA, Cerro Alfaro; LT, Late Tortonian sediments (Sandstones and marls); SB: Slump block; T, Terque; TA, Tabernas.

benthic foraminifera is evident (*Globigerina* sp. planktonic foraminifera and *Elphidium* sp. benthic foraminifera, Voermans, Baena, Ewert, et al., 1983), thus supporting the inclusion and mixing of Neogene material into this bed.

Breccia B30 constitutes an intermixture of different materials from both the metamorphic substrate and the Neogene sedimentary sequence. It is delimited upward by an erosional surface on which Quaternary sediments and calcretes have been deposited (Figure 6g).

Area of Extensive Brecciation at the Alhama de Almería “Slump Scar”: The Location of the Proposed Impact Structure

Breccias B31–B38 (Table 1) occur in relation with the “slump scar” on the northern slope of the Sierra de Gádor. Breccias B31–B36 (Figure 8a–f) are constituted by Triassic materials (Ladinian and Anisian) of the AC, that is, dolostones, limestones, and marls–argillites. Breccias B37 and B38 (Figure 8g,h) are polymict and matrix supported with angular clasts of black dolostone and, to a lesser extent, quartzites, phyllites, and limestone in a fine matrix of calcium carbonate.

In order to facilitate a comparison with the typical features of known impact structures, we separate the basement damage zone of the Alhama de Almería structure into two main areas:

The Crater Rim

The proposed crater rim (red solid semicircle in Figure 9a) is defined by the presence of an escarpment with a height that can be estimated at a minimum of 220 m, although in some areas, it can reach 350 m (Figure 10), and by the overturning of strata described by Sanz de Galdeano (1985) in the area of Cerro del Cuchillo and Cabezo Mesa Contrata (Figure 9b). Target strata in reversed order are also visible at the western rim (Figure 10) along the gravel road leading to localities B30 and B31 (Figure 9a).

Outside the rim scarp along the asphalt road A391 toward the south (i.e., toward locality B32 and Puerto de Enix; Figure 9a), an almost continuous, approximately 2 km long, road cut exposes a bed of polymict breccia resting on basement rocks. It is approximately 20 m thick in the parts nearest to the rim, where it also contains



FIGURE 4. (a) TA3. Megablocks in Tabernas Rambla in the eastern disturbed area in Late Tortonian 1 marls. Tilted megablock = late Tortonian 1 in Figure 2 (30SWF5128799298). (b) Detailed view of the TA8 megablock with partially rounded clasts of the Nevado-Filábride complex (graphite–micaschist, quartzites, and gneiss). (c) Background: 30 m high tilted megablocks and polymict breccia of Nevado-Filábride complex (graphite–micaschist, quartzites, and gneiss). Foreground: Brecciated dolomite of Alpujárride complex. Hammer: 28 cm. (d) Panoramic photograph of megablock zones. Rotated megablocks in zone 1: TA1 and TA2 and polymict breccia incorporated between megablocks (B1 and B2). (e) Megablock in zone 2 (CA1). (f) Megablock in zone 3. Note the houses for scale.

rotated blocks, mainly of dolomite, of up to several meters in diameter. The bed is gradually thinning outward along the road, and the clast size is decreasing to be dominated by coarse gravel at the termination of the bed.

The rim area is widely characterized by breccias such as the Breccia B30 described above. The clast lithologies are dolostones, phyllites, quartzites, gypsum, calcareous schists, with minor limestones and belong to the AC. This Betic basement was overlain by Miocene terrigenous marine deposits, however not of the thickness occurring in the basins. At the rim area, they all show a high degree of brecciation and mixing with the AC components (B30. Figure 6g). In addition, other breccias of the rim area may be clast-supported with almost no matrix, and with angular fragments of different sizes and lithologies (Figure 8a), as well as matrix supported with a more reddish color (Figure 8b). A further 400 m southwestward from the locality of Breccia 30 there is a transition of the

chaotic breccia into a set of meter-thick graded beds that fine upward into arenite (Figures S1 and S2).

The Crater Interior

In the profile by Sanz de Galdeano (1985) in Figure 9b, there are a set of seemingly upthrust blocks in the size order of half a kilometer wide and a couple of kilometers long. They occur between the rear escarpment of the “slump scar” and the northwestern end of the profile (i.e., between the suggested crater rim and the central uplift in Figure 9a). Similar, but smaller, terraces can be seen also along the western rim. The large coherent blocks consist of the same stacked Alpujárride units as the basement outside the structure. They are overlain by Miocene breccias, marine bioclastic conglomerates, and sandstones, which comprise clasts of the Alpujárride basement (Sola et al., 2018). The most representative characteristics of these materials is their intense brecciation giving rise to both clast-supported

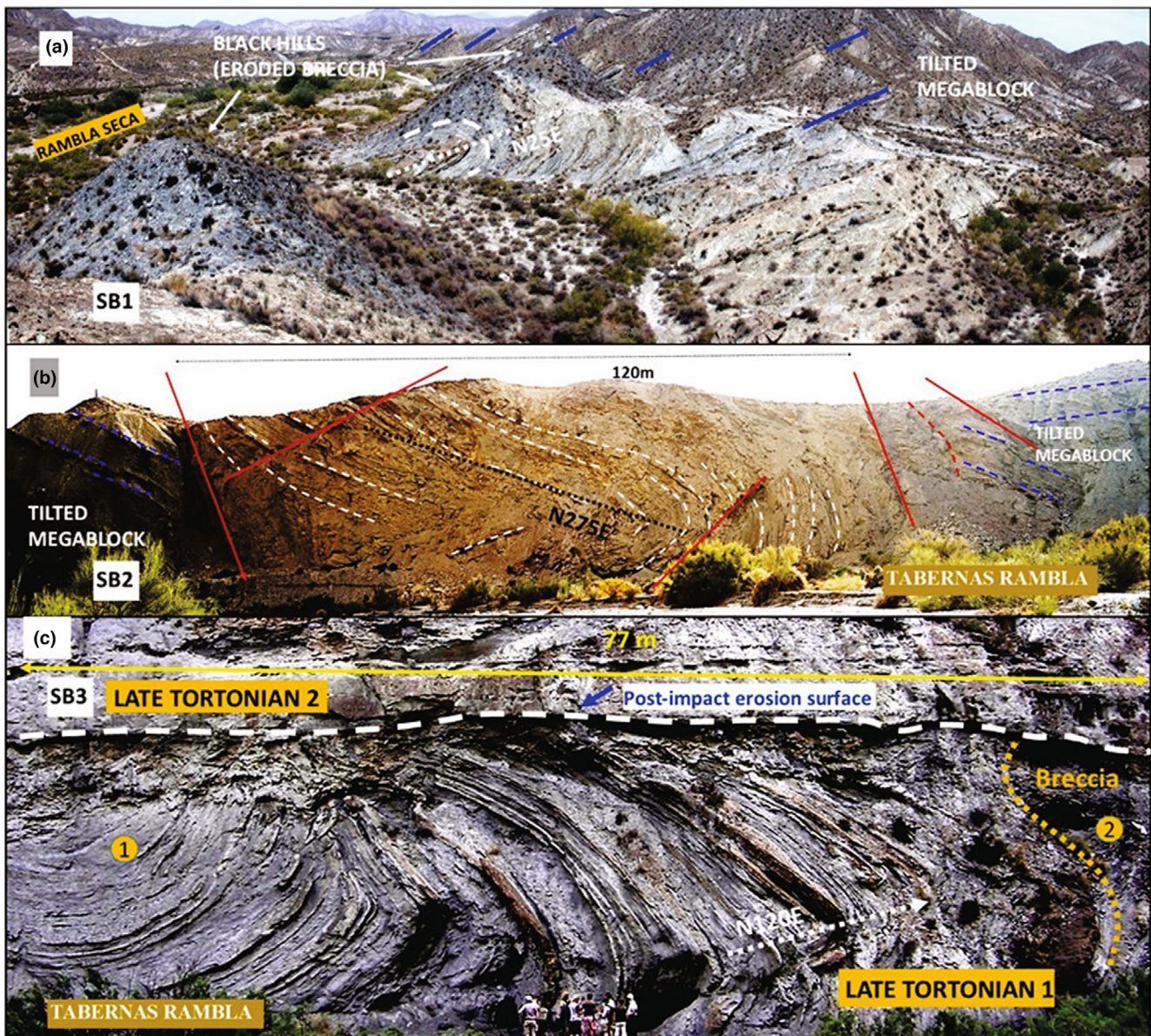


FIGURE 5. Panoramic photographs of plastically deformed megablocks within the slump deposits of the Gordo Megabed. Faults: red lines. Bedding: blue lines. (a) Slump block SB1, among rotated blocks and the remains of an eroded breccia made up of black hills of conical morphology. Red green: 130 m. (b) Slump block SB2, among tilted blocks. Faults: red lines. Bedding: blue lines. (c) Slump block SB3 forming an eye-catching feature within the megaslump (1). Stippled yellow line shows the contact between SB3 and polymict breccia with clasts of graphite–micaschist, quartzites, and gneiss (2). Stippled white line shows an erosion surface between the impact-related bed and postimpact sediments. Note persons for scale.

breccias (Figure 8c,d,f) and matrix-supported breccias (Figure 8e) of dolostone, limestone, and marl–argillites. In the southeastern part of the “slump scar,” Sola et al. (2018) have defined a chaotic melange of basement blocks, Miocene deposits, and marls laterally changing to a suite of redeposited materials. Notable is the presence of matrix-supported, polymict breccias with fragments of dolostone and, to a lesser extent, quartzites, in a fine matrix of calcium carbonate, that in places grade within a

few meters into muddy arenite with sporadic cm- to dm-sized clasts of mainly dolomite (Breccias 37 and 38 in Figure 8g,h. Figure S3).

In the northernmost area, to the west of Alhama de Almería (Figure 9a), the brecciation is notably lower than in the rest of the interior of the “slump scar.” There is also a rise in the topography, a relatively coherent mass of dolomite with the presence of potential shatter cones at the CIRERA HUMBRIÓN S.L. quarry (Figure 12), and

TABLE 2. Platinum group elements (PGEs) and Au concentration (ppb) in selected samples, determined using ICPMS.

Sample/Element	Au	Ir	Pd	Pt	Rh	Ru	Os	Re
Sample 4	204.32	2.66	5.15	2.33	nd	nd	66.94	2.33
B37	796.76	497.04	302.47	450.99	247.20	241.78	560.86	528.62
Limit UCC	1.5	0.022	0.52	0.51	0.06	0.34	0.05	0.198–0.4

Note: References: Hecht et al. (2010), Koeberl (2007), Peucker-Ehrenbrink and Bor-ming (2001), Rudnick and Gao (2003), Schmitz et al. (2006), Tagle et al. (2004), and Taylor and McLennan (1985, 1995). Sample 4: Figure 9a. B37: Figures 8g and 9a. Abbreviations: nd, not detected; UCC, upper continental crust concentration data.

indications for compressional tectonism not seen elsewhere along the Andarax fault zone (Marín-Lechado et al., 2007; Martín, 2006; Martínez Martos et al., 2017; Pedrera et al., 2012), that is, the 30 m high fold called “El Caracol,” Figure SM4. These observations prompt us to suggest this part to be the erosional remnants of a central uplift centered at 36°57'29" N, 2°34'42" W.

Shock Metamorphic Features and Geochemistry

Microscopic Shock Features

In two outcrops, we have collected 20 samples (e.g., samples 1 and 3 in Figure 6c,g) for making 20 thin sections. The systematic search for quartz grains with shock metamorphic features in samples 1 (B5) and 3 (B30), resulted in six quartz grains, five grains displaying one set of planar features and one grain with two sets (Figure 11a–d). Five grains are from sample 3 (B30) and one grain is from sample 1 (B5). The features are straight, parallel, sets of planes with a typical spacing between each plane of 1–5 μm . The planar features penetrate the entire grain in four cases, and in two cases, they were only visible near the grain boundary in part of the host grain. The features are generally fresh (Figure 11a,b), but occasionally decorated (Figure 11c,d), that is, lined by minute fluid inclusions. The planar features are oriented parallel to the $\{10\bar{1}4\}$ and $\{10\bar{1}3\}$ orientations in the quartz grain that has two sets of planar features.

Macroscopic Shock Features

A field survey in the quarry belonging to the company CIRERA HUMBRIÓN SL close to Alhama de Almería (Figures 3 and 9a) allowed the detection of potential shatter cones (Figure 12). The structures are pervasive of the lithology, which is a fine-grained, gray dolomite belonging to the Triassic basement rocks (AC). They are approximately 15 cm long, cup-shaped, and with a flat polygonal apical area.

Preliminary Geochemical Results from ICP-MS

Preliminary studies of the geochemistry of the marl in Sample 4 and the finer grained part of the graded Breccia 37 (Figure 8g, Table 2) performed at the Technical

Services of the University of Almería by ICPMS indicate the existence of a geochemical anomaly. The obtained values for PGEs are much higher than the background established for the upper continental crust, which supports our theory of the suggested impact structure. These samples are subject to continued analyses.

DISCUSSION

Geological and Geomorphological Evidence for an Impact Event

The geology and geomorphology of a 380 km² part of the northern area of the Sierra de Gádor mountain range and the Tabernas Basin show features that are shared with some impact structures in target settings comprised of relatively thick, poorly consolidated sedimentary deposits covering a more rigid basement, for example, the Chesapeake Bay Impact Structure (CBIS; e.g., Collins & Wünnemann, 2005; Collins et al., 2008; Ormö et al., 2009; hereafter CBIS) and the Wetumpka Crater (e.g., King Jr. & Ormö, 2011), both in the United States. Of course, the best indicator of an impact event is the perfectly preserved and exposed crater itself, but this is a rare occurrence on Earth, often only seen with marine-target craters that may be preserved thanks to being buried by continued marine sedimentation. Instead, the presumed impact site commonly is presented by a combination of evidence, often certain lithologies and combinations thereof. What first led us to suspect a potential formation by impact of the extensive area of brecciation on the northern slope of Sierra de Gádor and for the collapsed and slumped strata in the Tabernas Basin, was the anomalous occurrence polymict breccias over a wide area of the basin, and with basement clasts in a stratigraphic and geographic distribution anomalous with the known geological development of the basin. As the breccia shows no signs of being transported by water and occurs far from the mountain ranges bordering the basin, the interpretations of its formation are limited. Likewise, they show no evidence of metavolcanic clasts. Moreover, for its characteristics described above, it is possible to exclude tectonic, igneous (pyroclastic,

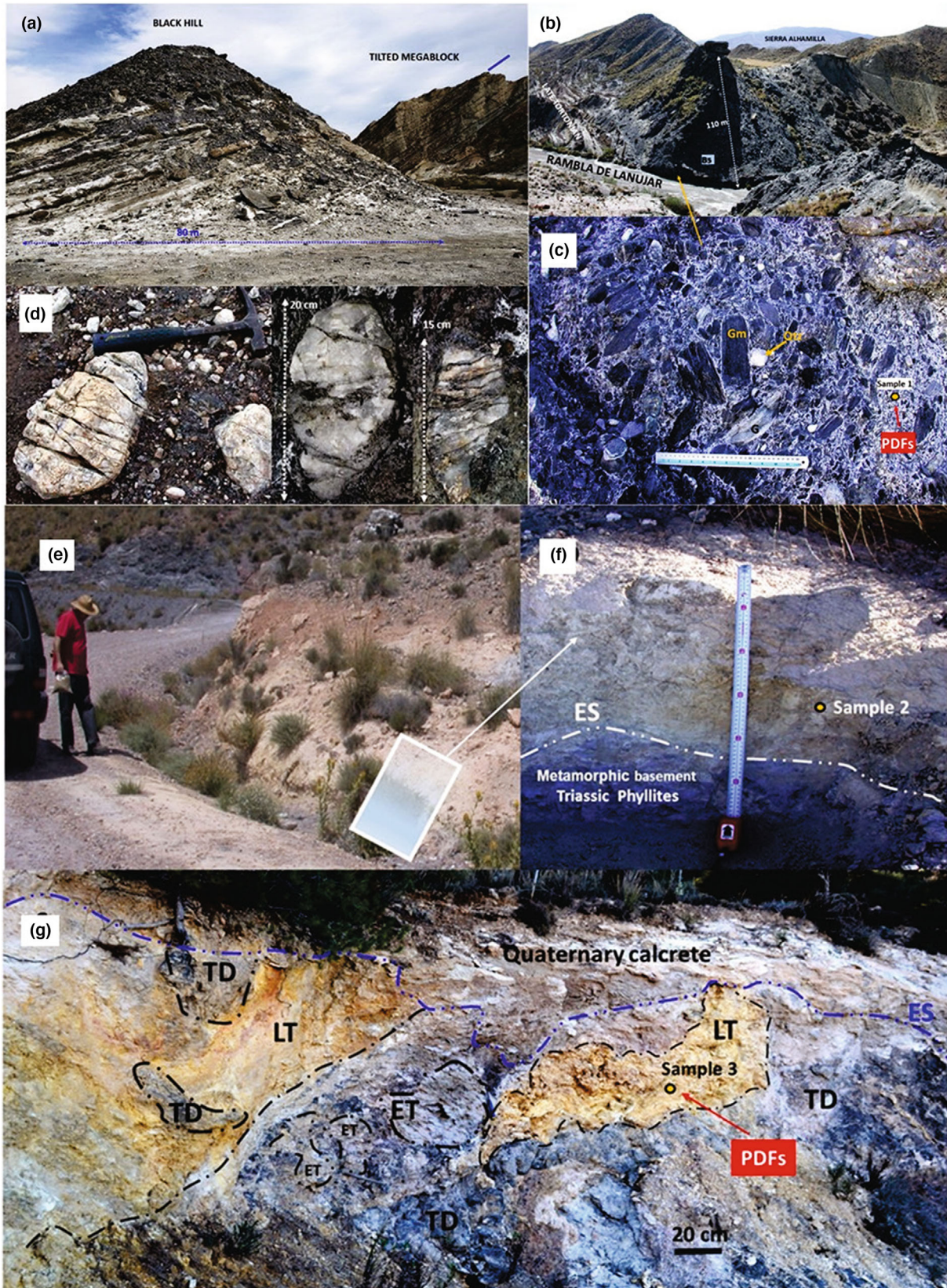


FIGURE 6. Examples of breccias. For locations, see Figure 3 and Table 1. (a) Example of *Black Hill* dark polymict breccia at locality B4 in Tabernas basin. It consists mainly of poorly consolidated coarse clastics where rain and wind have caused coarser fractions to be preserved as a surface residue. In the background, a similar dark polymict breccia occurs on top of stratified tilted megablock (30SWF4855597436). (b) Drone aerial photograph of breccia at locality B5. (c) Close-up of the polymict breccia at B5 in Lanújar Rambla, and location of Sample 1. The polymict breccia has mostly angular clasts of graphite-micaschist (GM), quartzite (Qtz), and gneiss (G) originating from the metamorphic basement of the area (30SWF4801797203). (d) Close-up of fractures in angular to subrounded clasts of quartzites within the polymict breccia at B5. (e) Outcrop of the Breccia 29 (30SWF5183992211). (f) Magnification of the inset in (e) and location of Sample 2. (g) Breccia 30 (30SWF3350888570) and location of Sample 3 analyzed for shock evidence (likely PDFs shown in Figure 11). ES, Erosion surface, white line in (f) and blue line in (g); ET, early Tortonian (marls with silex); LT, late Tortonian (sandstones and yellow marls); TD, Triassic dolomites.

volcanic, or intrusive) and hydrothermal breccia formation (Figure 6c).

Likewise, in the area of the previously proposed “slump scar” at Alhama de Almería, there are observations that are inconsistent with a gravity-driven formation and that instead suggest a formation by a cosmic impact:

- Existence of a topographic rise with overturned basement strata marking a typical crater rim in the landscape (Figures 9a and 10).
- Existence of a several meters thick bed of polymict breccias that in places extend up to a couple of kilometers outside the elevated rim in the opposite direction of the suggested flow of the submarine slump (i.e., opposite to the direction of gravity).
- Extensive distribution of both autochthonous and allochthonous breccias both within the area of the suggested impact structure (i.e., the “slump scar”) and over a waste area of the Tabernas Basin (Figures 3a,d and 9a). These types of lithologies are probably the most abundant and often the most noticeable type of impact-produced rock in established impact structures (e.g., French & Koeberl, 2010).
- Conspicuous fractures in quartz clasts (Figure 6d) that are reminiscent of fractures noted to occur in clasts at impact craters and impact-related deposits, for example, the Vakkejokk Breccia ejecta layer (Ormö et al., 2017).
- Planar deformation features (PDFs) in quartz grains from lithologies (breccias) that show no signs of being beds by reworked distal ejecta layers from older impact events.
- Shatter cones at the center of the basement structure in fine-grained, gray dolomite.
- Geochemical anomaly in Au and PGEs (Ru, Rh, Pd, Os, Ir, Re, and Pt; Table 2) of levels diagnostic for impact structures (French & Koeberl, 2010). The occurrence of the geochemical anomaly in material reminiscent of graded resurge deposits at known marine-target impact craters provides additional support for the impact hypothesis as it is in such

deposits traces of the projectile and other highly shocked material are accumulated (cf. Alwmark & Schmitz, 2007; Sturkell, 1998).

An important feature of breccias B29 and B30 for the impact hypothesis is the anomalous position they occupy geographically, altitudinally, and stratigraphically, since they present neither vertical nor horizontal stratigraphic continuity (alignment) with the surrounding substrate. Another significant feature is the high degree of dislocation of the materials: broken strata, and a strong heterogeneity in the mixture of both basement (basal) and Miocene sediments, which have been deposited, in both cases, over an erosional surface. These features could be compatible with a proximal ejecta layer, which in B30 is further supported by the presence of shock metamorphic features as expected for ejecta deposits (cf. Osinski et al., 2013).

Megablock zones have been described in many impact structures formed in stratified targets such as the CBIS with megablocks ranging 0.5–2 km in size (Poag et al., 2004), Wetumpka Crater with tens of meters large sedimentary megablocks in a transcrater slide unit of ~100 m thickness (King Jr., 1997; King Jr. et al., 2002, 2006, 2015; King Jr. & Ormö, 2011), Ries crater ranging from 60 to 150 m (e.g., Collins et al., 2008; Sarv et al., 2019), and in impact craters on Mars where they are described as layered megablocks with thicknesses on meter to decameter scales (Caudill et al., 2012).

The formation of megablocks can begin already during the crater excavation stage, in which large blocks of the target may be both collapsing inward and downward in a zone just outside the position of the transient crater rim as exemplified at Ries (Collins et al., 2008), as well as thrown outward together with other ejecta of various fragment sizes. However, as exemplified by Wetumpka and CBIS, the relatively thick, and poorly consolidated sediments of the upper target strata caused an extensive collapse and slumping under influence of gravity that continued relatively long after the end of crater excavation (e.g., Horton Jr. et al., 2006; King et al., 2006 and references therein).

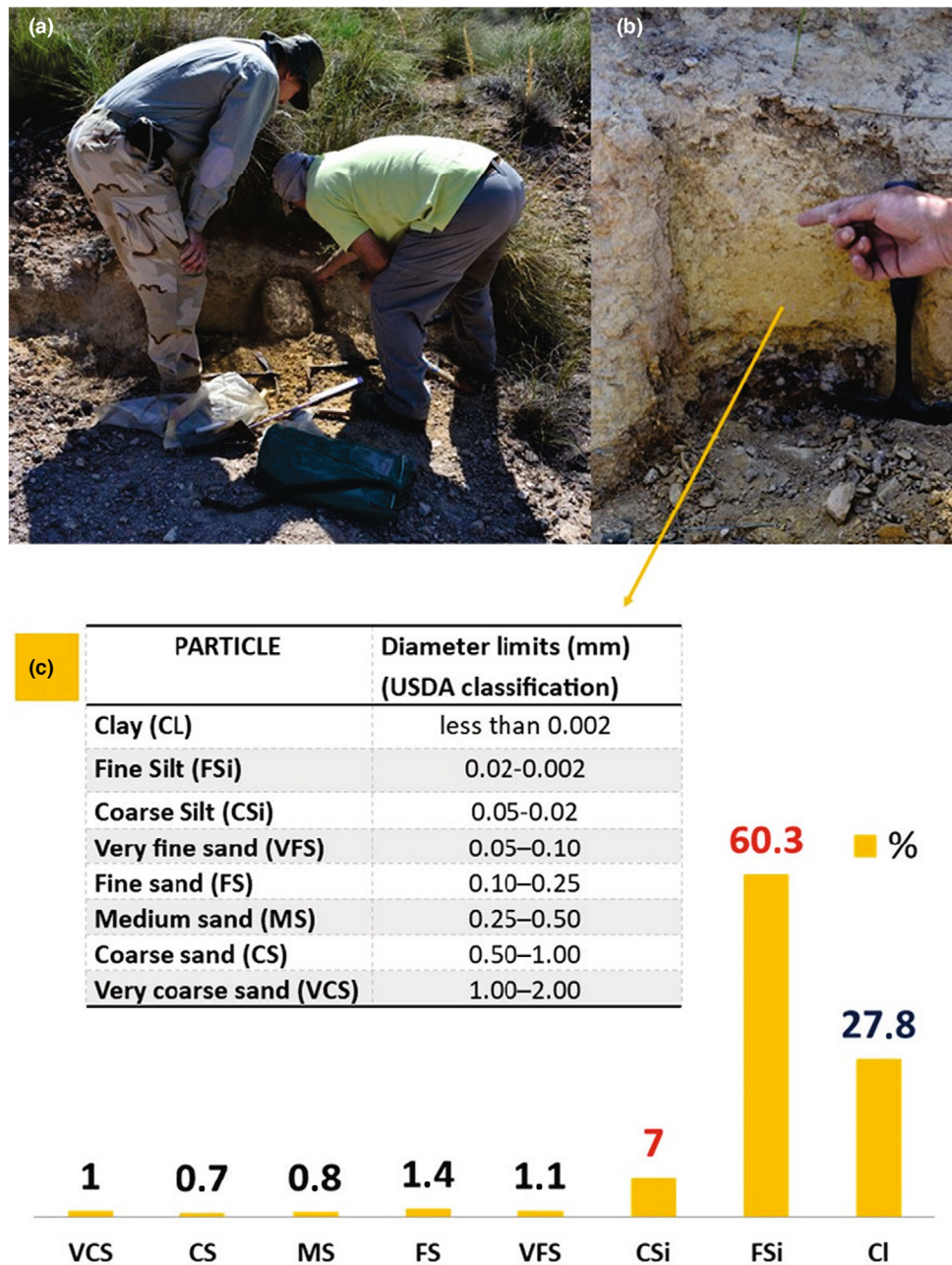


FIGURE 7. Breccia 29. (a) Sampling of the breccia. (b) Close-up of sampled material. (c) Texture and composition determined according to Marañés et al. (1998). Cl, clay; CS, coarse sand; CSi, coarse silt; FS, fine sand; FSi, fine silt; MS, medium sand; VCS, very coarse sand; VFS, very fine sand.

These observations, together with their close relation to the polymict breccias B1–B28 and the tilted, and sometimes contorted megablocks of the Gordo megabed seem reminiscent of the situation described at the Wetumpka crater, CBIS, and to some extent also the Ries crater. Likewise, the formation of what we here define as “Plastically Deformed Megablocks” has in the context of impact cratering been described by Melosh (1977) and Collins et al. (2012) as a consequence of gravitational

collapse during the final stage of crater modification in complex craters.

Thus, we will here focus on comparisons with these structures in order to relate our observations to the suggested impact hypothesis. However, to prove the impact origin of a suspected impact structure evidence in the form of diagnostic shock metamorphic features and/or a meteoritic component are needed (French & Koeberl, 2010). Hence, lithologies potentially analogous to impactites

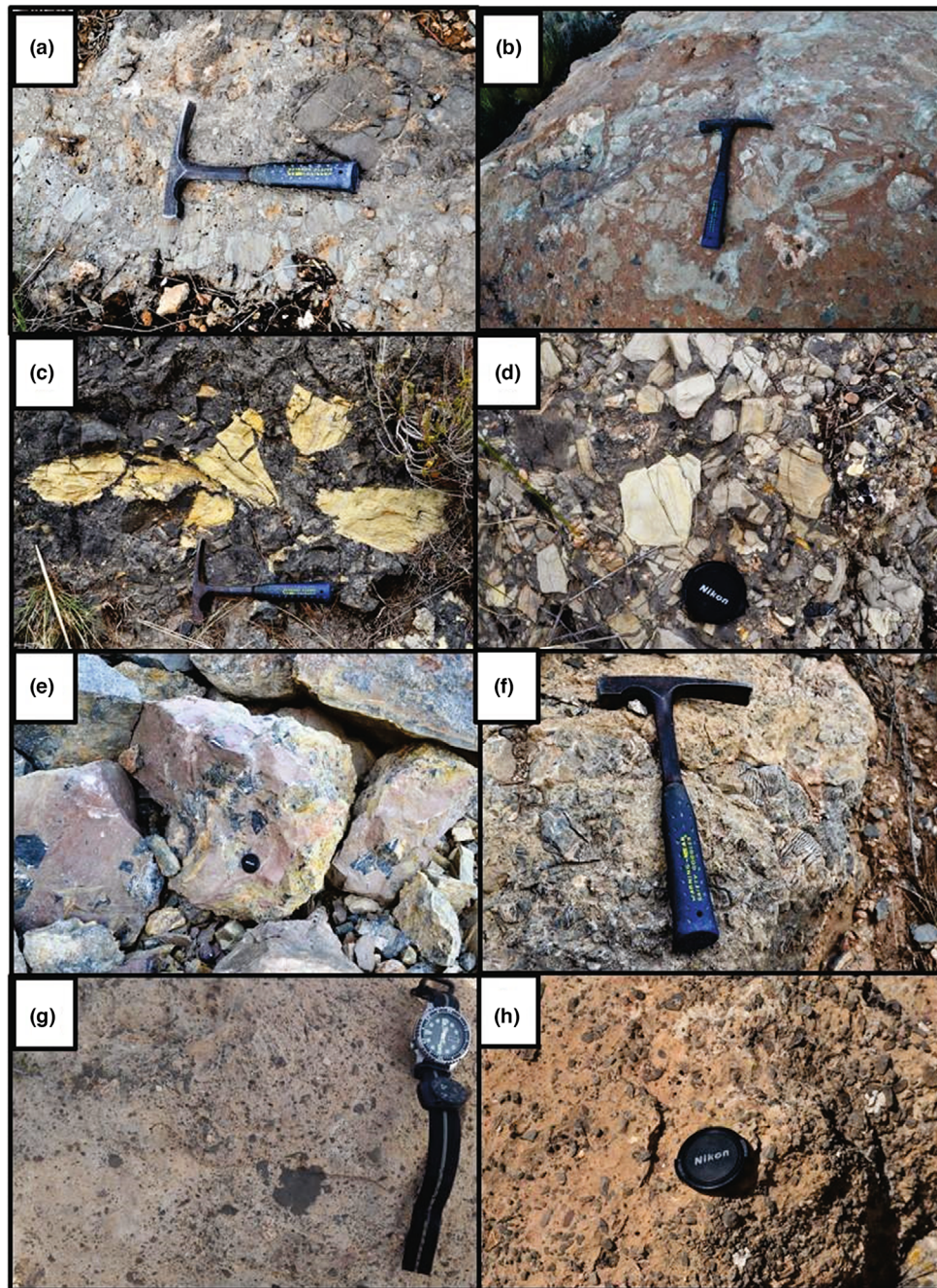


FIGURE 8. Examples of the intense brecciation and mixing of the materials (For locations, see Figure 9) located both suggested outer rim (a, b) and inner rim (c–h). (a) Clast-supported breccia with angular fragments of different sizes and rock types (black and gray dolostones). (b) Matrix-supported breccia with angular fragments of different sizes and lithologies (limestones and black dolostones), with red, fine-grained matrix. (c) Polymict breccia with black brecciated dolostones (Ladinian) with marl-argillite clasts (Anisian). (d) Clast-supported breccia with angular fragments of black dolostone, limestone, and marl limestones. (e) Matrix-supported polymict breccia with angular fragments different sizes of black dolostone “facies franciscana” and marl limestones with red, fine-grained matrix, here occurring in blocks quarried by the Cirera Humbrión SL company, Alhama de Almería. (f) Clast supported breccia with angular clasts of dolostone “facies franciscana” (millimeter or centimeter alternation of black bands with white bands, which gives them a “zebra-shaped” appearance). (g, h) Graded matrix-supported polymict breccias with fragments of dolostone and, to a lesser extent, quartzites, phyllites, and limestones in a fine matrix of calcium carbonate. Hammer: 28 cm. Lens cap: 5 cm. Diameter of wristwatch: 4.5 cm.

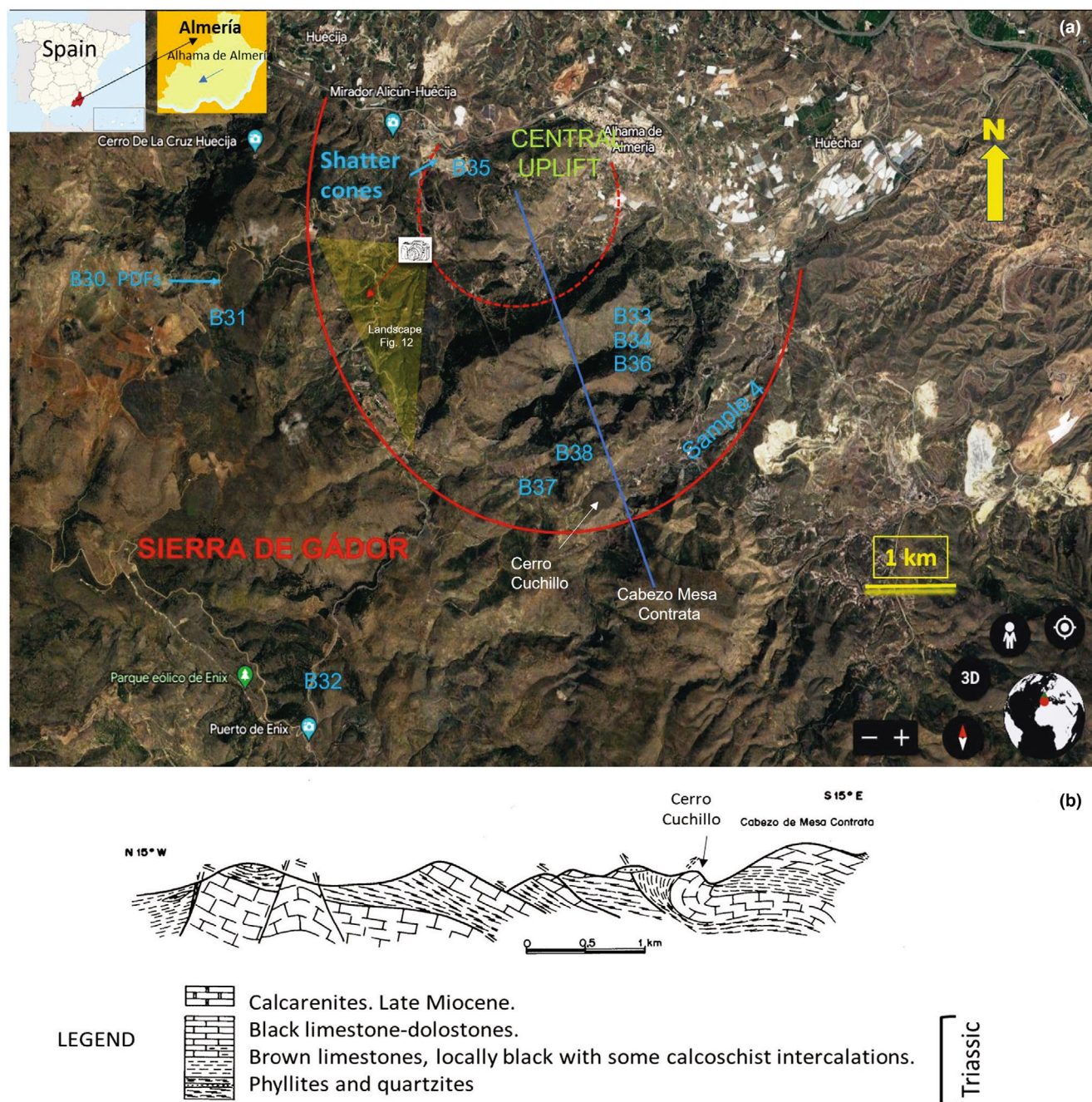


FIGURE 9. (a) Location of the proposed crater area, overlaid on Google Earth V 9.186.0.0. Imagen date 17/06/2015–15/04/2022. Inst. Geogr. Nacional. Eye alt. 15 km. Data SIO, NOAA, U.S. Navy, NGA, GEBCO. <http://www.earth.google.com>. Accessed March 20, 2023. (b) Previously published cross section of the Alhama de Almería-Cabezo Mesa Contrata area with conspicuous overturning of strata in the area of Cerro del Cuchillo and Cabezo de Mesa Contrata (adapted from Sanz de Galdeano, 1985). Red line: Suggested crater rim. Red dotted line: Limit of central uplift. Blue line: Location of the cross section by Sanz de Galdeano (1985). B30: Figure 6a. B31: Figure 8a. B32: Figure 8b. B33: Figure 8c. B34: Figure 8d. B35: Figure 8e (quarry company CIRERA HUMBRIÓN S.L.). B36: Figure 8f. B37: Figure 8g (Table 2). B38: Figure 8h. Sample 4: Marl outcrop in chaotic melange (Table 2).

known to express shock metamorphic features were a priority in our survey.

Planar deformation features in quartz are oriented parallel to rational crystallographic planes in the host

crystal (see e.g., French & Koeberl, 2010). Most commonly, PDFs in quartz are oriented to planes of low Miller-Bravais indices, such as $\{0001\}$, $\{10\bar{1}4\}$, ω $\{10\bar{1}3\}$, π $\{10\bar{1}2\}$, and r, z $\{10\bar{1}1\}$. The PDFs that we

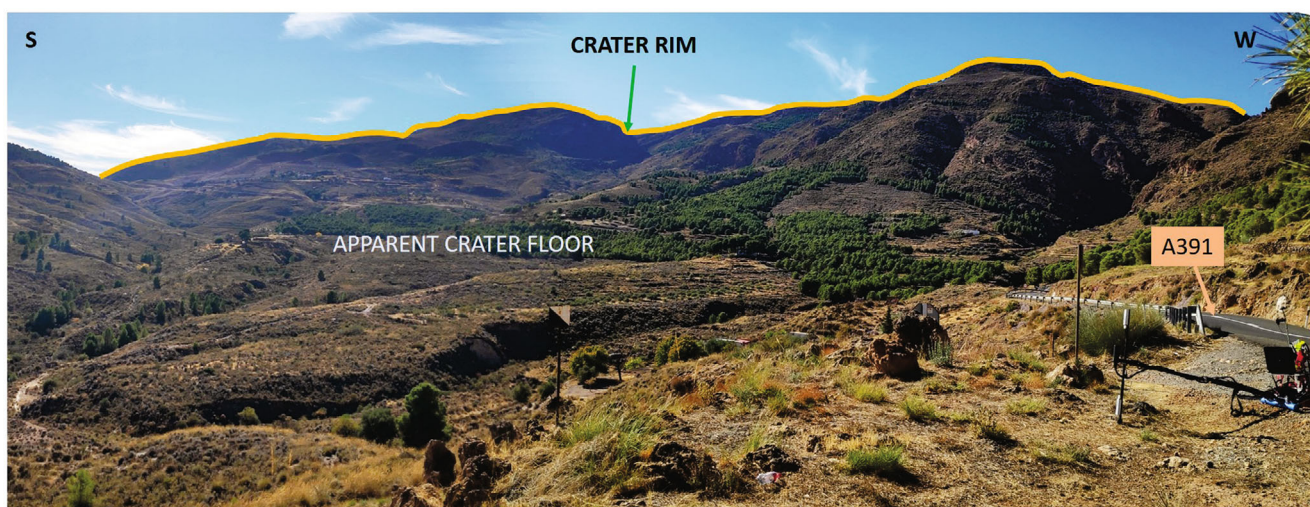


FIGURE 10. General panorama of the proposed basement crater (“nested crater”) with the rim in the background. The difference in height (up to 350 m) between the apparent crater floor and the crater rim can be seen. Note country road for scale.

observed in samples 1 (Breccia B5) and 3 (Breccia B30) are oriented parallel to crystallographic planes $\{10\bar{1}4\}$, $\omega\{10\bar{1}3\}$, $r, z\{10\bar{1}1\}$, and $s\{11\bar{2}1\}$, respectively. However, by optical microscopy and stereographic projection template, due to quartz crystal symmetry, it is in fact only possible to index multiple sets of PDFs (i.e., at least two sets of features are needed). This means that in our case, only one grain, the grain displaying two sets, one set oriented parallel to $\omega\{10\bar{1}3\}$ and one set oriented parallel to $\{10\bar{1}4\}$, could be properly indexed.

Thus, further investigations, hopefully revealing more shock metamorphic features, are needed before the structure can be definitely confirmed as being the result of an impact. The low number of shocked quartz grains recovered in our analysis means that we cannot exclude that the one grain was not transported to the present locality (see e.g., Cavosie et al., 2010). But it can also be an effect of the suggested relatively small size of the actual impact structure in the basement (~5 km, Table 3) compared to the large volumes of mobilized sediments (Figure 13). In potential analogy with Wetumpka, the polymict breccias holding the shocked material in the Alhama de Almería structure would represent the “surficial polymict impact breccia” known for its relatively low shock pressures, and with a proposed origin as near-field ejecta (King Jr. et al., 2015).

The presence of potential shatter cones in basement rocks at what we propose to be the exposed parts of a central uplift of the suggested impact structure in the basement is a further indication for an impact formation of the Alhama de Almería structure (Figure 12, Figures 3 and 9a for location). Unfortunately, the features shown

in Figure 12 have, since the photo was taken, been removed by the quarrying. As the fine-grained host material is favorable for the formation of shatter cones, future field surveying may be able to confirm the existence. Nevertheless, in light of the indicative, presence of shock metamorphic features, in particular quartz shocked grains in lithologies analogous to known impactites, their composition, appearance, stratigraphic position and geographical distribution, as well as the other sedimentological, stratigraphic, petrographic and geomorphological observations, lead us to propose the existence of a possible impact structure in the study area. In our model, the crater is in parts preserved under slump breccias and postimpact materials north of the Andarax fault zone (Marín-Lechado et al., 2007; Martín, 2006; Martínez Martos et al., 2017; Pedrera et al., 2012), but with its main parts exposed as a deeply eroded structure exposed on the flank of Sierra de Gádor just to the south of the normal fault (Figures 3, 9a and 13).

The suggested damaged (collapsed) zone within the Tabernas Basin extend to approximately 22 km along the length of the basin (Table 3, Figure SM5). Due to the elongated shape of the basin, the collapse does not form a circular feature. Nevertheless, the dimensions of the damaged (collapsed) zone would place it in the size range of impact structures such as the Ries (cf. Collins et al., 2008 and references therein). As the Ries also formed in a stratified target with sedimentary rock covering a crystalline basement would suggest it to be a natural choice of comparison with the Alhama de Almería structure. However, in the comparison with Ries, the relatively small diameter of the actual basement

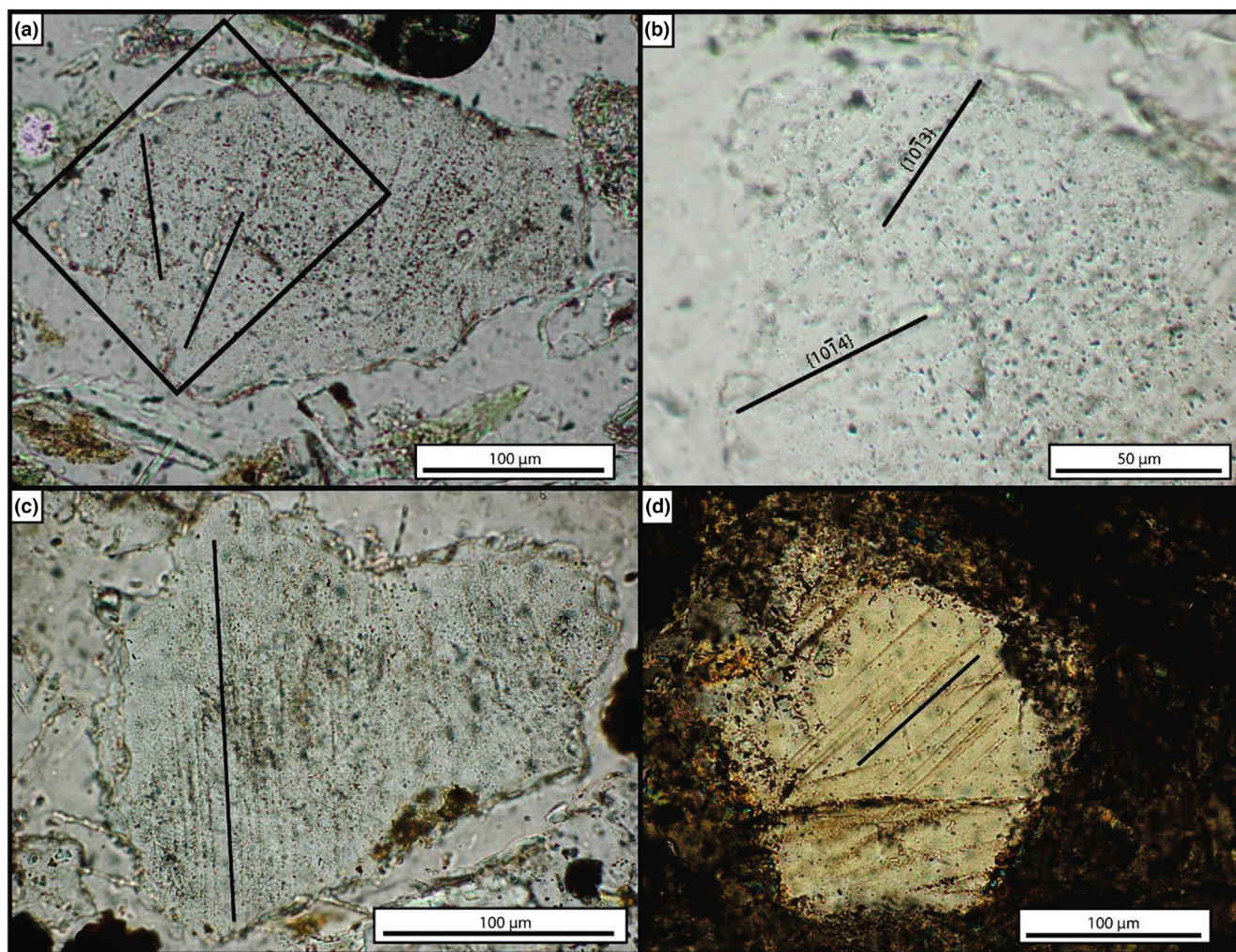


FIGURE 11. Thin section photomicrograph of quartz grains of Sample 3 from Breccia 30 (a–c, uncrossed polars) and Sample 1 from Breccia 5 (d, crossed polars). (a) Quartz grain displaying two sets of undecorated PDFs, one set oriented parallel to ω $\{10\bar{1}3\}$ equivalent orientations and one set oriented parallel $\{10\bar{1}4\}$ equivalent orientations. (b) Close-up of part of the grain in a (black rectangle in plate a). Note that the set oriented parallel $\{10\bar{1}4\}$ equivalent orientations are hardly visible in the image but are clearly observable under the U-stage microscope. (c) Quartz grain with one set of decorated PDFs. (d) Quartz grain with one set of partly decorated PDFs of Sample 1 from Breccia 5.

structure (~ 5 km) to that of the zone of collapsed and slumped sedimentary strata suggests the Alhama de Almería structure to represent a much lesser magnitude event than Ries. This is also supported by the relatively scarce shock metamorphic features and melted material at Alhama de Almería compared to the Ries. Instead, our model is mainly based on two examples of impact structures, CBIS and Wetumpka that have a geology and geomorphology much affected by extensive collapse and slumping of a thick upper layer of poorly consolidated, mainly clastic sediments covering a rigid, crystalline basement (Figure 14). At the Ries, the sedimentary strata were more consolidated not allowing the same extensive collapse (cf. Collins et al., 2008).

The Formation of the Alhama de Almería Structure as a Consequence of a Marine Hypervelocity Impact

At the buried, approximately 80 km wide, marine-target CBIS, the collapse of the somewhat over 400 m thick layer of sediments caused the crater to expand to over twice the diameter it would have had in a target without these significant strength variations (Collins & Wünnemann, 2005). This caused a concentric (“inverted sombrero”) shape of the crater with a wide, shallow, outer crater developed in the sedimentary strata surrounding an ~ 38 km wide, ~ 1.6 km deep, nested crater in the crystalline basement (e.g., Horton Jr. et al., 2006). It is known that layering of the target may



FIGURE 12. Potential shatter cones in gray dolomite (Alhama de Almería, quarry of the company Cirera Humbrión S.L.). The apexes (pointing toward the upper right corner of the photo) are cut, showing a flat polygonal cross section. The striae appear to form a “horsetail” pattern (cf., Kenkmann et al., 2016; Pen: 14 cm).

TABLE 3. Estimated characteristics of various parameters of the crater model.

Estimates of the dimensions and main characteristics of the model	
Rim diameter of nested crater	5 km
Rim diameter of outer crater	22 km
Depth of the crater	1 km
Diameter central uplift	2.4 km
Pre-impact target stratigraphy:	Betic metamorphic basement:
Impact lithologies	<ul style="list-style-type: none"> • Alpujárride Complex (AC): Limestones and Dolostones. Triassic • Nevado-Filábride Complex (NFC): Graphite–micaschist, quartzites, and gneiss. Paleozoic • Ladinian + Anisian. Black dolostones, limestones, and marl limestones
	<ul style="list-style-type: none"> • Late Tortonian 1: Turbidites systems, and submarine fans. Alternating sand, sandstones, and silty marls
	<ul style="list-style-type: none"> • Early Tortonian + Serravallian: Submarine fans and coastal platform. Gray conglomerates sandstones and marls
Environment	Marine continental shelf
Age of impact	~8 Ma (Late Tortonian)

suppress the formation of a central uplift (Hopkins et al., 2019). However, the relatively large nested crater at CBIS shows a well-developed central uplift. The shallow outer crater constituting the “brim” of the “sombbrero” is known as the annular trough (Powars & Bruce, 1999) and the deep nested crater contains a moat that encircles the central uplift (Horton Jr. et al., 2004, 2005). The impact-related crater-fill materials in the CBIS include suevitic crystalline clast breccia and megablocks in the nested crater, impact-modified autochthonous to parautochthonous

sediments in the annular trough, and allogenic sediment clast breccia deposited over the entire crater and its vicinity (Horton Jr. et al., 2006). The deformed sediments in the annular trough show a decreasing amount of transport, disintegration, and rotation of blocks away from the crater center indicating a headward expansion of the slump process. This megablock slump unit is overlain by the allogenic sediment clast breccia, which is suggested to great extent to be a resurge deposit due to returning seawater at this shallow-marine impact (e.g.,

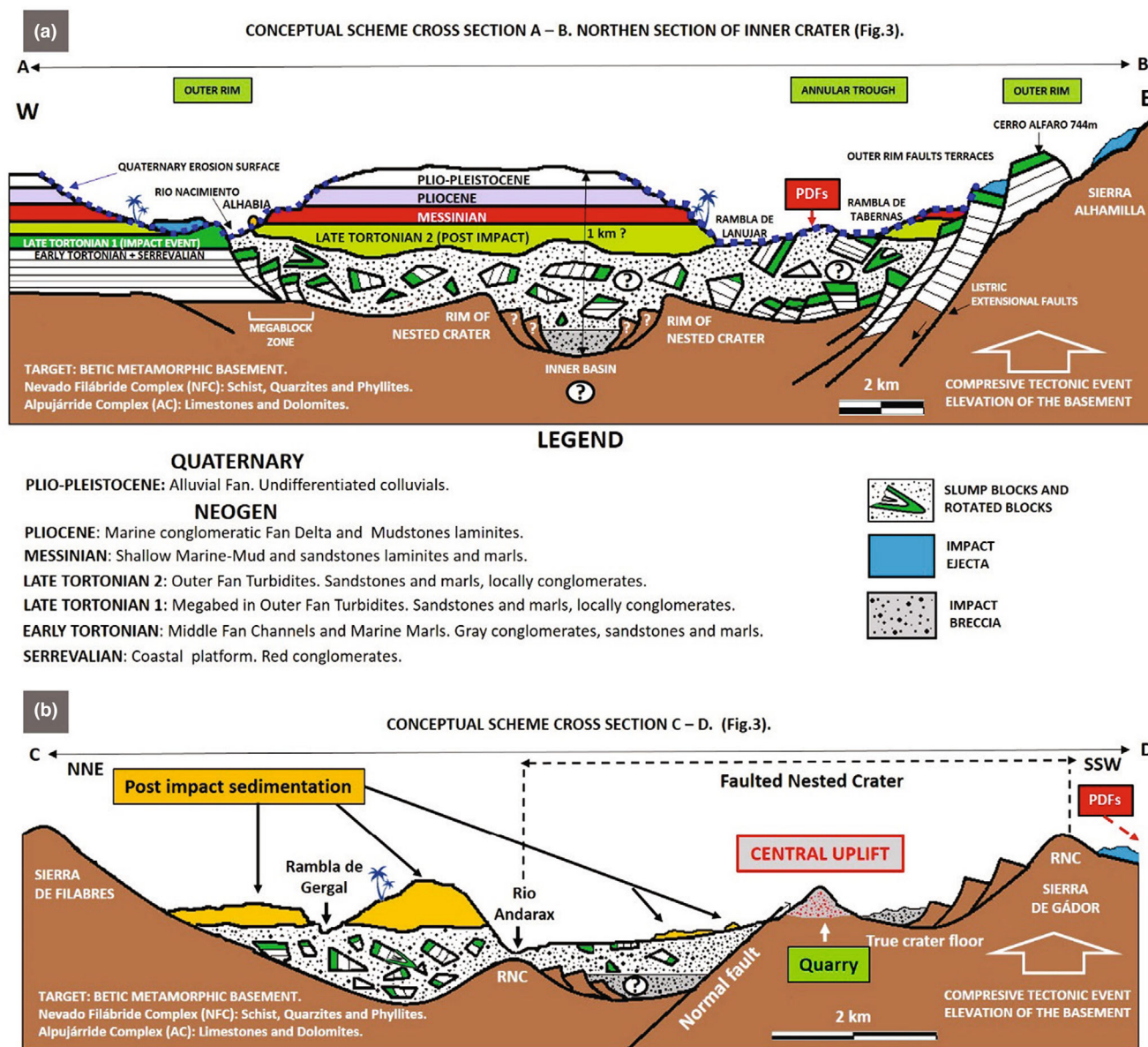


FIGURE 13. Conceptual scheme of the suggested impact structure with a nested crater developed mainly in the basement (largely exposed on the flank of Sierra de Gádor), and adjacent extensive collapse of parts of the Alhabia–Tabernas Basin sediments developing an “outer crater” (see CBIS analogue in Figure 14). (a) An E–W transversal cross section A–B (see Figure 3) of the sedimentary Alhabia–Tabernas Basin (Figure 1). Vertical scale five times exaggerated. (b) Transversal cross section C–D (see Figure 3) passing the exposed parts of the basement crater as well as the down-faulted, hypothetical continuation (marked with?) below the collapsed basin sediments. Vertical scale three times exaggerated. RNC denotes “rim of nested crater.” The central uplift is inferred from topography, stratigraphic relations of target lithologies, and the location of the potential shatter cones (Figure 12). Sequence of events: (1) Uplift Sierra de los Filabres, Sierra Nevada, Sierra de Gádor, and formation of Tabernas Basin. (2) Impact into a shallow-marine setting at the boundary between the sediment-filled Alhabia–Tabernas Basin and the thinning sediments and basement of the rising Sierra de Gádor. (3) Continued uplift of Sierra de Gádor along the normal fault north of the central uplift and dislocation of the crater.

Ormö et al., 2009). Thus, the ejecta was strongly reworked by the resurge and blended with rip-up material from the slump unit (Dypvik et al., 2018; Ormö et al., 2009).

At the likewise shallow-marine, approximately 7 km wide, Wetumpka impact structure, the layer of seawater

and sediments varied in thickness over the target area similar to CBIS (e.g., King Jr. et al., 2002, 2003). However, the relatively thinner upper layer of sediments and seawater allowed a significant development of a basement crater rim. Nevertheless, on the seaward side,

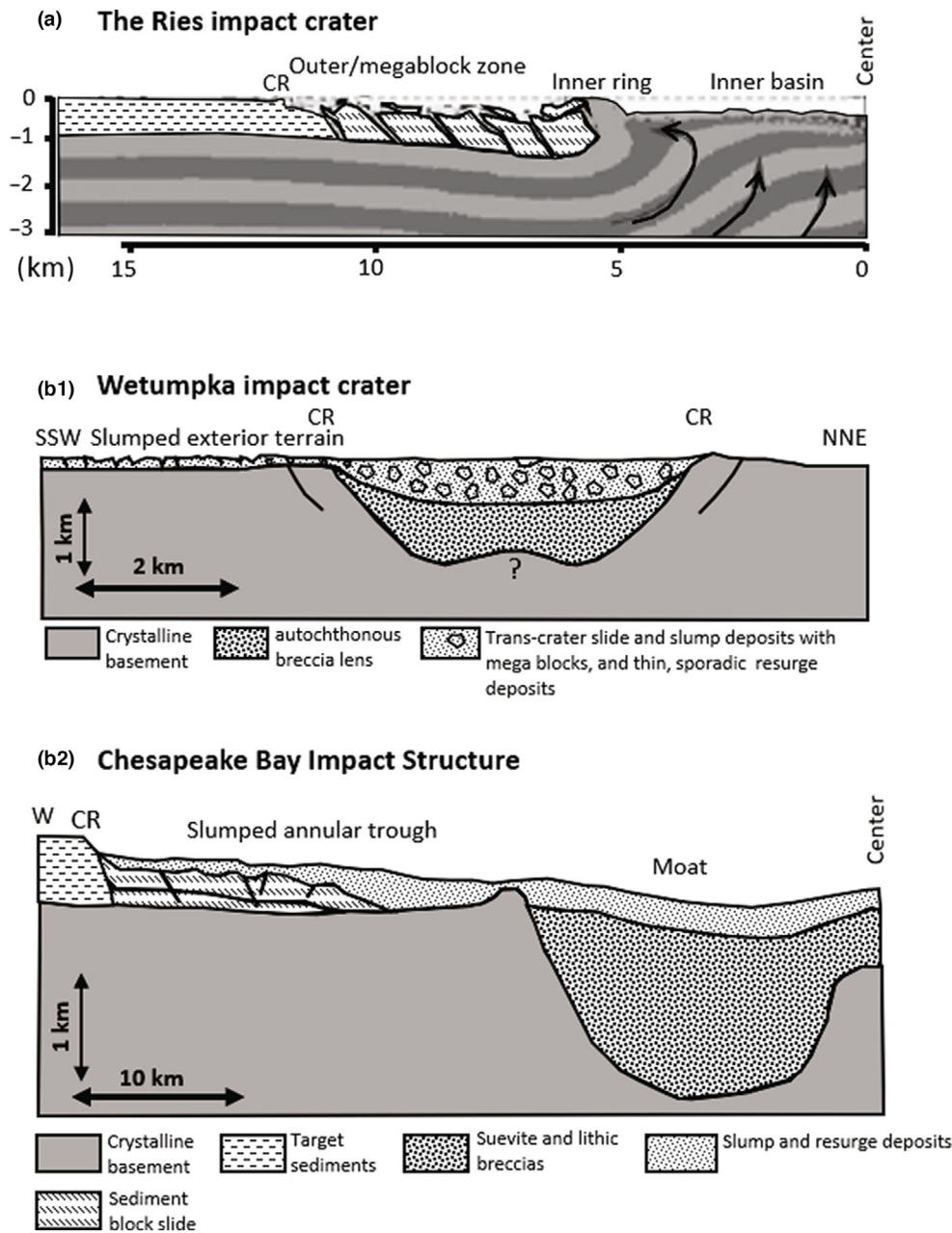


FIGURE 14. Cross sections of craters of relevance for structural comparisons with the proposed Alhama de Almería impact structure. (a) In the Ries impact crater, the outer zone (also called megablock zone) formed in relatively competent sedimentary rock during the crater excavation and early modification just outside the transient crater rim, which comes to form the “inner ring” in mainly basement rock. Note that this is not a “peak ring” formed by collapse of an overshooting central peak. Crater infill is not shown in this figure (modified from Wünnemann et al., 2005; information also from Collins et al., 2008). (b) At the Wetumpka crater and the Chesapeake Bay impact structure (CBIS) poorly consolidated sediments begin to collapse during crater excavation, but the collapse continues as an extensive slumping for a relatively long time as indicated by the stratigraphic position of the deposits from oceanic resurge (see Ormö et al., 2009). In our model of the Alhama de Almería structure in Figure 13, we find Wetumpka and CBIS to be better analogs for the understanding of the formation of the nested basement crater and the outer slump zone in sedimentary strata. CR denotes the position of the published apparent crater rim for all craters.

where the sediments and water layer were thicker, the basement crater rim became unstable and collapsed back into the crater (King et al., 2006). In the parts with

crystalline crater rim development, further expansion of the crater by slumping was prevented. However, on the side with the opening in the rim, the exterior target

sediments layer became unstable and slid inward into the basement crater allowing a headward expansion by subhorizontal sliding of sedimentary megablocks to a distance of about one crater radius beyond the basement crater rim. Thus, the crater obtained a “baseball cap” morphology rather than a complete “inverted sombrero” (King Jr. & Ormö, 2011). Therefore, it is also in this sense to be considered as a concentric crater with an outer crater in the sedimentary target strata and a nested, basement crater, like CBIS. As the chaotic slumped terrain outside the crater rim does not include the whole periphery of the crater it is not, like at CBIS, called an annular trough. Instead, King Jr. et al. (2003) describe it as the “extrastructure terrain.”

Inside the inferred location of the collapsed basement, the slumped sedimentary target strata that collapsed into the open void now consist of megablocks that have undergone intensive soft-sediment deformation (contorted bedding and clastic dikes) and peripheral disaggregation (King Jr. & Ormö, 2011). This slump-displaced megablock unit crops out over most of the infrastructure area. Where it is not exposed, it is covered by Quaternary terrace deposits, patchy occurrences of resurge deposits, or a surficial polymict impact breccia unit, which due to its composition, and content of shocked material is interpreted as late modification stage slumping of proximal ejecta from the impact structure’s rim (King Jr. et al., 2015). There is no clear indication for a central uplift in the Wetumpka crater. Early models were based on the assumption that the crystalline target would follow the “standards,” that is, that in terrestrial structures, the transition from simple to complex craters occurs with a diameter of approximately 4 km in massive crystalline rocks, and around 2 km in sedimentary rocks (e.g., French, 1998). However, King Jr. et al. (2015) find it possible that the crystalline rock, perhaps being more highly weathered than previously assumed, would have behaved physically more like sedimentary rock, resulting in a significantly more shallow crater and could even possess a small, submerged central uplift.

We interpret the approximately 5 km wide area of the previously proposed “slump scar” on the boundary between the northern slope of Sierra de Gádor and the Alhabia–Tabernas Basin to be the exposed part of the actual “nested” crater of the Alhama de Almería impact structure (Figure 9a). The extensive brecciation, overturned strata, uplifted basement with potential shatter cones at the center, marked geochemical anomaly of the platinum group elements (PGEs) and Au as well as extensive polymict breccia layer with shock features (Breccia B30) overlying basement rock outside the rim are altogether what to be expected for an impact crater of this size. Due to the later uplift of the parts of the crater developed in the basement south of the normal fault

(Figure 13b), much of the inferred breccia lens would have eroded out toward the Andarax river exposing the breccia infill, and even the true crater floor and the central uplift. Nevertheless, the graded polymict breccias and arenites (Breccias B37 y B38, NE Cerro Cuchillo) inside the suggested crater strongly resemble resurge deposits described from other marine-target crater (e.g., Ormö et al., 2007, 2009, 2021). Such deposits are known to represent the last of the impact-related infill of the crater and are, thus, suggesting a relatively good level of preservation of some parts of the crater interior. They are also known to be the primary location for highly shocked and projectile material, at least in small- and medium-sized craters (e.g., the Lockne Crater Alwmark & Schmitz, 2007; Sturkell, 1998).

Based on the observations in the study area compared to similar features at the CBIS and Wetumpka (Figure 14), a conceptual east–west cross section of the collapsed terrain of the Tabernas Basin, as well as NNE–SSW profile of the suggested, partially exposed basement impact structure is drawn in Figure 13, the transects of which appear in Figure 3 (A–B, C–D).

The cross section A–B in Figure 13a puts our observations along the Tabernas Basin into the context of impact-generated collapse of thick, poorly consolidated strata exterior to an impact crater in analogy with CBIS and Wetumpka. When extrapolating from the exposed parts of what we suggest to be the basement (nested crater) south of the normal fault north of the Central Uplift (Figure 13b), we can assume that some of the northern parts of the crater are still buried under several hundreds of meters of the known slump breccias and postimpact sediments in the Tabernas Basin north of the fault. This is indicated as a “nested crater” in profile A–B in Figure 13a although its dimensions in this part are unknown. As the proposed ejecta layer at the SSW end of profile C–D rest directly on basement rocks, and the polymict breccias occurring within the exposed crater mainly contain clasts from the basement, we assume that there was a thinning of the basin sediments in the direction of the Sierra de Gádor already before the uplift of the southern part of the basement crater. Nevertheless, toward the basin in the north, the thick sediment sequence would have caused an instability of the rim, and consequently the extensive exterior collapse, in analogy with the formation of the “extrastructure terrain” at Wetumpka.

The target schist at the Alhama de Almería structure is in many ways similar to that at the Wetumpka crater (e.g., weathered and relatively ductile), and there are also extensive dolomites within the target basement rocks. Thus, it is possible that there could be a central uplift at the center of the suggested crater just south of the normal fault (Figure 13b). This is supported by the observation

of the possible shatter cones in the dolomite quarry at this location. Shatter cones are primarily observed at the central uplift in impact structures of this size although they may also occur in other parts of the structure such as the ejecta layer (Osinski & Ferrière, 2016).

Stratigraphically above the suggested impact-related units, to the N and the W, large parts of the Alhabia–Tabernas basin are covered with upper Neogene, Tortonian, and Messinian sediments that include breccias, conglomerates, and sands, overlain by silts, sands, and gypsum. In the silt beds, there are spectacular slumps, probably seismites, indicating the tectonic instability that existed during the upper Neogene times (Braga et al., 2003). Pliocene–Quaternary is represented by red conglomerates, sandstones, and silts. Younger Quaternary deposits correspond to different fluvial terraces, generally formed by conglomerates and sands (Braga et al., 2003; Kampschuur et al., 1975; Sanz de Galdeano et al., 2006; Velando et al., 1979; Voermans, Baena, Ewert, et al., 1983; Voermans, Baena, Martínez, et al., 1983).

Paleoenvironment of the Inferred Impact Site and Implications for the Dating of the Event

About 8 million years ago (late Miocene), the configuration of emerged and submerged land around the littoral margin of Almería was similar to that of today, but not identical: the sea extended through the territory of today's Tabernas Desert up to the foot of the Sierra de los Filabres in whose borders coral reefs of this age formed, today reliably marking the position of the ancient coastline (Braga et al., 2003). On the slopes of this ancient sea, submarine fans deposited a thick and extensive sedimentary package of material transported by rivers from the eroded emerging relief (Braga et al., 2003; Velando et al., 1979; Voermans, Baena, Ewert, et al., 1983). Later, some 7 million years ago (Upper Miocene), the Sierra Alhamilla and Sierra de Gádor were uplifted, closing a narrow and elongated, marine intermontane basin between this new relief to the south, and Sierra de los Filabres to the north (Braga et al., 2003).

The estimated date of the putative impact event (~8 Ma), which coincides with a strong tectonic activity and the presence of very representative seismites, has been estimated by biostratigraphic criteria (Kleverlaan, 1987; Poisson et al., 1999; Sola et al., 2018).

The paleogeographic setting at the estimated age of the putative impact event would indicate a target water depth of possibly as much as 600 m (Poisson et al., 1999). However, the impact occurred on a shallow platform separating the already emerged Sierra de los Filabres and Sierra Nevada to the N (micaschists and quartzites) and Sierra de Gádor to the S (limestones and dolomites)

(Figure 1). Thus, the platform constitutes a high floor with some modestly emerged relief (Braga et al., 2003; Voermans, Baena, Martínez, et al., 1983). The Andarax River Valley (Figure 3) in the Alhabia Basin (Figure 1) is a deep and subsiding depression through which a narrow sea extended to the W (Braga et al., 2003; Voermans, Baena, Martínez, et al., 1983).

Resurge deposits are significant of marine-target craters (e.g., Örmö & Lindström, 2000). Nevertheless, the hitherto only discovered potential resurge deposits within the exposed part of the basement impact structure are thin, and the polymict ejecta on top of the slump breccias of the Tabernas Basin show no sign of major reworking. Altogether, this supports a very shallow target water depth. After the suggested impact, during uppermost Tortonian (late Tortonian 2 in Figure 13a) and Messinian, the area was uplifted gradually, since no sediments are deposited in the core of the Sierra de Gádor, while in the Alhabia Basin, the facies present are continental to the W and regressive marine, lagoon, brackish, and deltaic to the E (Braga et al., 2003; Voermans, Baena, Martínez, et al., 1983). However, the seemingly strong uplift of the exposed parts of the impact structure in the basement rocks of Sierra de Gádor indicates that this mountain range was uplifted relatively more strongly.

CONCLUSIONS

The geology of the Tabernas basin shows lithologies (polymict breccia deposits) and geomorphological features that are unique for the region and that have provoked the suggestion of various models for their formation by workers for decades. In light of new findings of six shocked quartz grains with potential shock metamorphic features (PDFs) in marls and polymict breccias in anomalous stratigraphic, geographic, and altitudinal positions, a 5 km wide area with extensive basement brecciation delimited by an overturned rim, a continuous several meters thick bed of breccia (i.e., ejecta) outside this rim, marked geochemical anomaly of the PGEs and Au as well as potential shatter cones at the center of the basement structure, we here propose the formation the Alhama de Almería structure by an impact event during the late Tortonian. A comparison with established impact structures showing similar geological features (e.g., CBIS and Wetumpka) that have a geology and geomorphology much affected by extensive collapse and slumping of a thick upper layer of poorly consolidated, mainly clastic sediments covering a rigid, crystalline basement, suggests that the impact caused collapse of large parts of the Tabernas Basin, and that the impact likely occurred in a shallow aquatic paleoenvironment.

Acknowledgments—We express our gratitude to Gordon Osinski (AE), David T. King, and one anonymous reviewer for their constructive comments and suggestions, which significantly improved the quality of this manuscript. This work was supported grant PID2021-125883NB-C22 by the Spanish Ministry of Science and Innovation/State Agency of Research MCIN/AEI/10.13039/501100011033 and by “ERDF A way of making Europe” (Jens Ormö, Sebastián Tomás Sánchez Gómez, Juan Antonio Sánchez Garrido); an International postdoc grant from the Swedish Research Council, grant 2017-06388 (Sanna Holm-Alwmark); the Swedish Research Council, grant 621-2012-4504, and the Crafoord Foundation, grant 20140617 (Carl Alwmark); and grant UAL2020-RNM-B1980 Convocatoria 2020 Proyectos I + D + I Marco Programa Operativo Feder—Andalucía 2014–2020 (Juan Antonio Sánchez Garrido, Sebastián Tomás Sánchez Gómez, Jens Ormö, Sanna Holm-Alwmark, Carl Alwmark, and Robert Lilljequist) and company CIRERA HUMBRIÓN S.L. (Juan Antonio Sánchez Garrido, Sebastián Tomás Sánchez Gómez).

Editorial Handling—Dr. Gordon Osinski

REFERENCES

- Akkerman, I. H., Maier, G., and Simon, O. J. 1980. On the Geology of the Alpujarride Complex in the Western Sierra de Las Estancias (Betic Cordilleras, SE Spain). *Geologie Mijnb* 59: 363–374.
- Alwmark, C., and Schmitz, B. 2007. Extraterrestrial Chromite in the Resurge Deposits of the Early Late Ordovician Lockne Crater, Central Sweden. *Earth and Planetary Science Letters* 253: 291–303. <https://doi.org/10.1016/j.epsl.2006.10.034>.
- Berggren, W. A., Hilgen, F. J., Langereis, C. G., Kent, D. V., Obradovich, J. D., Rafi, I., Raymo, M. E., and Shackleton, N. J. 1995. Late Neogene Chronology: New Perspectives in High-Resolution Stratigraphy. *GSA Bulletin* 107: 1272–87. [https://doi.org/10.1130/0016-7606\(1995\)107<1272:LNCNPI>2.3.CO;2](https://doi.org/10.1130/0016-7606(1995)107<1272:LNCNPI>2.3.CO;2).
- Braga, J. C., Baena, J., Calaforra, J. M., Coves, J. V., Dabrio, C., Feixas, C., Fernández, J. M., et al. 2003. *Geology of Arid Zone of Almería, South East Spain. An Educational Field Guide*. TECNA S.L. 165. <https://www.juntadeandalucia.es/medioambiente/portal/documents/20151/5395847/Geologia-entorno-arido-Almeria-ENG.pdf/26f01f00-fc4e-9414-d17d-dddd4f4b3182?t=1609313452850>.
- Caudill, C. M., Tornabene, L. L., McEwen, A. S., Byrne, S., Ojha, L., and Mattson, S. 2012. Layered Mega Blocks in the Central Uplifts of Impact Craters. *Icarus* 221: 710–720. <https://doi.org/10.1016/j.icarus.2012.08.033>.
- Cavosie, A. J., Quintero, R. R., Radovan, H. A., and Moser, D. E. 2010. A Record of Ancient Cataclysm in Modern Sand: Shock Microstructures in Detrital Minerals from the Vaal River, Vredefort Dome, South Africa. *Geological Society of America Bulletin* 122: 1968–80. <https://doi.org/10.1130/B30187.1>.
- Cloetingh, S., Van der Beek, P. A., Van Rees, D., Roep, T. B., Biermann, C., and Stephenson, R. A. 1992. Flexural Interaction and the Dynamics of Neogene Extensional Basin Formation in the Alboran-Betic Region. *Geo-Marine Letters* 12: 66–67.
- Collins, G., and Wünnemann, K. 2005. How Big was the Chesapeake Bay Impact? Insight from Numerical Modeling. *Geology* 33: 925. <https://doi.org/10.1130/G21854.1>.
- Collins, G. S., Kenkmann, T., Osinski, G. R., and Wünnemann, K. 2008. Mid-Sized Complex Crater Formation in Mixed Crystalline-Sedimentary Targets: Insights from Modeling and Observation. *Meteoritics & Planetary Sciences* 43: 1955–77. <https://doi.org/10.1111/j.1945-5100.2008.tb00655.x>.
- Collins, G. S., Melosh, H. J., and Osinski, G. R. 2012. The Impact-Cratering Process. *Elements* 8: 25–30. <https://doi.org/10.2113/gselements.8.1.25>.
- Crespo-Blanc, A., Comas, M., and Balanyá, J. C. 2016. Clues for a Tortonian Reconstruction of the Gibraltar Arc: Structural Pattern, Deformation Diachronism and Block Rotations. *Tectonophysics* 683: 308–324. <https://doi.org/10.1016/j.tecto.2016.05.045>.
- Cronin, B. T. 1994. Channel-Fill Architecture in Deep Water Sequences: Variability, Quantification and Applications. Unpublished PhD thesis, University of Wales, UK, 332 p.
- Cronin, B. T. 1995. Structurally-Controlled Deep-Sea Courses: Examples from the Miocene of Southeast Spain and the Alboran Sea, Southwest Mediterranean. In *Characterization of Deep Marine Clastic Systems. Geological Society Special Publication*, edited by A. J. Hartley, and D. P. Prosser, vol. 94, 115–135. London: Geological Society. <https://doi.org/10.1144/GSL.SP.1995.094.01.10>.
- Dabrio, C. J., Martín, J. M., and Megías, A. G. 1985. The Tectosedimentary Evolution of Mio-Pliocene Reefs in the Province of Almería. In *6th European Regional Meeting of Sedimentologists, Excursion Guidebook*, edited by M. D. Milá, and J. Rosell, 269–305. Lleida: IAS.
- Dabrio, C. J., Mateu, E., and Martín, J. M. 1981. The Coral Reef of Njar, Messinian (Uppermost Miocene), Almería Province, S.E. Spain. *Journal of Sedimentary Research* 51: 521–539. <https://doi.org/10.1306/212F7CCA-2B24-11D7-8648000102C1865D>.
- Dypvik, H., Gohn, G. S., Edwards, L. E., Horton, J. W., Jr., Powars, D. S., and Litwin, R. J. 2018. Chesapeake Bay Impact Structure—Development of “Brim” Sedimentation in a Multilayered Marine Target. *Geological Society of America Special Paper* 537: 1–68. <https://doi.org/10.1130/2018.2537>.
- Engelhardt, W. V., and Bertsch, W. 1969. Shock Induced Planar Deformation Structures in Quartz from the Ries Crater, Germany. *Contributions to Mineralogy and Petrology* 20: 203–234.
- Ferrière, L., Morrow, J. R., Amgaa, T., and Koeberl, C. 2009. Systematic Study of Universal-Stage Measurements of Planar Deformation Features in Shocked Quartz: Implications for Statistical Significance and Representation of Results. *Meteoritics & Planetary Science* 44: 925–940. <https://doi.org/10.1111/j.1945-5100.2009.tb00778.x>.
- French, B. M. 1998. *Traces of Catastrophe: A Handbook of Shock-Metamorphic Effects in Terrestrial Meteorite Impact Craters*. Houston, TX: Lunar and Planetary Institute. Contribution CB-954.
- French, B. M., and Koeberl, C. 2010. The Convincing Identification of Terrestrial Meteorite Impact Structures: What Works, What Doesn't, and Why. *Earth-Science Reviews* 98: 123–170. <https://doi.org/10.1016/j.earscirev.2009.10.009>.

- García-García, F., Fernández, J., Viseras, C., and Soria, J. M. 2006. High Frequency Cyclicity in a Vertical Alternation of Gilbert-Type Deltas and Carbonate Bioconstructions in the Late Tortonian, Tabernas Basin, Southern Spain. *Sedimentary Geology* 192: 123–139. <https://doi.org/10.1016/j.sedgeo.2006.03.025>.
- García-Tortosa, F. J., and Sanz de Galdeano, C. 2007. Evidencias geomorfológicas de actividad tectónica cuaternaria en el frente montañoso del borde sur de Sierra Nevada: La falla normal de Laujar de Andarax. Cuaternario y geomorfología. *Revista de la Sociedad Española de Geomorfología y Asociación Española para el Estudio del Cuaternario* 21: 101–112.
- Gómez Pugañe, M. T., Rubatto, D., Fernández Soler, J. M., Jabaloy, A., López Sánchez, V., González Lodeiro, F., Galindo Zaldívar, J., and Padrón Navarta, J. A. 2012. Late Variscan Magmatism in the Nevado-Filábride Complex: U-Pb Geochronologic Evidence for the Pre-Mesozoic Nature of the Deepest Betic Complex (SE Spain). *Lithos* 146: 93–111. <https://doi.org/10.1016/j.lithos.2012.03.027>.
- Harvey, A. M. 2001. Uplift, Dissection and Landform Evolution: The Quaternary. In *A Field Guide to the Geology and Geomorphology of the Neogene Sedimentary Basins of the Almería Province, SE Spain*, edited by A. E. Mather, J. M. Martín, A. M. Harvey, and J. C. Braga, 227–239. Oxford: Blackwell.
- Harvey, A. M., Foster, G., Hannam, J., and Mather, E. A. 2003. The Tabernas Alluvial Fan and Lake System, Southeast Spain: Applications of Mineral Magnetic and Pedogenic Iron Oxide Analyses Towards Clarifying the Quaternary Sediment Sequences. *Geomorphology* 50: 151–171. [https://doi.org/10.1016/S0169-555X\(02\)00212-X](https://doi.org/10.1016/S0169-555X(02)00212-X).
- Haughton, P. D. W. 2000. Evolving Turbidite Systems on a Deforming Basin Floor, Tabernas, SE Spain. *Sedimentology* 47: 497–518. <https://doi.org/10.1046/j.1365-3091.2000.00293.x>.
- Hecht, L., Reimold, W. U., Sherlock, S., Tagle, R., Koeberl, C., and Schmitt, R. 2010. New Impact-Melt Rock from the Roter Kamm Impact Structure, Namibia: Further Constraints on Impact Age, Melt Rock Chemistry, and Projectile Composition. *Meteoritics & Planetary Science* 43: 1201–18. <https://doi.org/10.1111/j.1945-5100.2008.tb01123.x>.
- Hopkins, R., Osinski, G. R., and Collins, G. S. 2019. Formation of Complex Craters in Layered Targets with Material Anisotropy. *Journal of Geophysical Research: Planets* 124: 349–373. <https://doi.org/10.1029/2018JE005819>.
- edited by Horton, J. W., Jr., Powars, D. S., and Gohn, G. S. 2005. Studies of the Chesapeake Bay Impact Structure—The USGS-NASA Langley Corehole, Hampton, Virginia, and Related Coreholes and Geophysical Surveys <https://doi.org/10.3133/pp1688>. U.S. Geological Survey Professional Paper 1688. Reston, VA: U.S. Geological Survey, 464 p.
- Horton, J. W., Jr., Gohn, G. S., Powars, D. S., Jackson, J. C., Self-Trail, J. M., Edwards, L. E., and Sanford, W. E. 2004. Impact Breccias of the Central Uplift, Chesapeake Bay Impact Structure: Initial Results of a Test Hole at Cape Charles, Virginia (Abstract). *Geological Society of America Abstracts with Programs* 36: 266.
- Horton, J. W., Jr., Vanko, D. A., Naeser, C. W., Naeser, N. D., Larsen, D., Jackson, J. C., and Belkin, H. E. 2006. Postimpact Hydrothermal Conditions at the Central Uplift, Chesapeake Bay Impact Structure. 37th Lunar and Planetary Science Conference. <https://www.lpi.usra.edu/meetings/lpsc2006/pdf/1842.pdf>.
- IGME. 2023. Cartographic viewer, IGME (Instituto Geológico y Minero de España) <http://info.igme.es/visorweb/>.
- IGN. 2023. Cartographic Viewer LIDAR Map. IGN (Instituto Geográfico Nacional). Viewer IBERPIX 4 <https://www.ign.es/iberpix2/visor/>.
- Jong, K. D., and Bakker, H. 1991. The Mulhacen and Alpujarride Complex in the Eastern Sierra de los Filabres, SE Spain: Litho-Stratigraphy. *Geologie en Mijnbouw* 70: 93–103.
- Kampschuur, W., García, G., Vissers, R., Verbug, J., Wolff, R., Perconing, E., Martínez, C., Fernández, M. C., and Martínez, J. 1975. Hoja 1030 (Tabernas) del Mapa Geológico de España E. 1:50.000. Mapa y memoria. IGME.
- Kenkmann, T., Hergarten, S., Kuhn, T., and Wilk, J. 2016. Formation of Shatter Cones by Symmetric Crack Bifurcation: Phenomenological Modeling and Validation. *Meteoritics & Planetary Science* 51: 1519–33.
- King, D., Ormö, J., Petruny, L. W., and Neathery, T. L. 2006. Role of Water in the Formation of the Late Cretaceous Wetumpka Impact Structure, Inner Gulf Coastal Plain of Alabama, USA. *Meteoritics & Planetary Science* 41: 1625–31. <https://doi.org/10.1111/j.1945-5100.2006.tb00440.x>.
- King, D. T., Jr. 1997. The Wetumpka Impact Crater and the Late Cretaceous Impact Record. In *The Wetumpka Impact Crater and Related Features*, edited by T. L. Neathery, D. T. King, Jr., and W. Lorraine, vol. 34C, 25–56. Alabama Geological Society Guidebook. <https://webhome.auburn.edu/~kingdat/wetumpkawebpage3.htm#:~:text=The%20Wetumpka%20impact%20crater%20in, stratigraphic%20uplift%20resulting%20from%20impact>.
- King, D. T., Jr., Morrow, J. R., Petruny, L. W., and Ormö, J. 2015. Surficial Polymict Impact Breccia Unit, Wetumpka Impact Structure, Alabama: Shock Levels and Emplacement Mechanism. In *Large Meteorite Impacts and Planetary Evolution V*. Geological Society of America, Vol. 518, edited by G. R. Osinski, and D. A. Kring. Beaverton, OR: Ringgold Inc. [https://doi.org/10.1130/2015.2518\(10\)](https://doi.org/10.1130/2015.2518(10)).
- King, D. T., Jr., Neathery, T. L., and Petruny, L. W. 2003. Crater-Filling Sediments of the Wetumpka Marine-Target Impact Crater (Alabama, USA). In *Cratering in Marine Environments and on Ice*, edited by H. Dypvik, M. J. Burchell, and P. Claeys, 97–113. Berlin: Springer-Verlag.
- King, D. T., Jr., Neathery, T. L., Petruny, L. W., Koeberl, C., and Hames, W. E. 2002. Shallow-Marine Impact Origin of the Wetumpka Structure (Alabama, USA). *Earth and Planetary Science Letters* 202: 541–49. [https://doi.org/10.1016/S0012-821X\(02\)00803-8](https://doi.org/10.1016/S0012-821X(02)00803-8).
- King, D. T., Jr., and Ormö, J. 2011. The Marine-Target Wetumpka Impact Structure Examined in the Field and by Shallow Core-Hole Drilling. *Geological Society of America, Special Paper* 483: 287–296. [https://doi.org/10.1130/2011.2483\(19\)](https://doi.org/10.1130/2011.2483(19)).
- Kleverlaan, K. 1987. Gordo Megabed: A Possible Seismitic in a Tortonian Submarine Fan, Tabernas Basin, Province Almería, Southeast Spain. *Sedimentary Geology* 51: 165–180. [https://doi.org/10.1016/0037-0738\(87\)90047-9](https://doi.org/10.1016/0037-0738(87)90047-9).
- Kleverlaan, K. 1989a. Three Distinctive Feeder-Lobe Systems within One Time Slice of the Tortonian Tabernas Fan, SE Spain. *Sedimentology* 36: 25–45. <https://doi.org/10.1111/j.1365-3091.1989.tb00818.x>.
- Kleverlaan, K. 1989b. Neogene History of the Tabernas Basin (SE Spain) and its Tortonian Submarine Fan Development. *Geologie en Mijnbouw* 68: 421–432.

- Kleverlaan, K. 1989c. Tabernas Fan Complex: A Study of a Tortonian Fan Complex in a Neogene Basin, Tabernas, Province of Almería, SE Spain. PhD thesis, University of Amsterdam, the Netherlands, 97 p.
- Koeberl, C. 2007. The Geochemistry and Cosmochemistry of Impacts. In *Treatise of Geochemistry*, edited by A. Davis, vol. 1, 1.28.1–1.28.52. New York, NY: Elsevier. <https://doi.org/10.1016/B978-008043751-4/00228-5>.
- Marañés, A., Sánchez Garrido, J. A., de Haro, S., Sánchez Gómez, S. T., and del Moral, F. 1998. *Análisis de Suelos: Metodología e Interpretación*. Servicio de Publicaciones Universidad de Almería. 184.
- Marín-Lechado, C., Galindo-Zaldívar, J., Rodríguez-Fernández, L. R., and Pedrera, A. 2007. Mountain from Development by Folding and Crustal Thickening in the Internal Zone of the Betic Cordillera-Alborán Sea Boundary. *Pure and Applied Geophysics* 166: 1–21. <https://doi.org/10.1007/s00024-006-0157-4>.
- Martín, I. 2006. Las Unidades Internas del sector de la Sierra de Gádor: Estructura y Evolución Geodinámica. Tesis Doctorales, Universidad de Alicante.
- Martín, J. M., and Braga, J. C. 2001. Shallow Marine Sedimentation. In *A Field Guide to the Neogene Sedimentary Basins of the Almería Province, South-East Spain*, edited by A. Mather, J. M. Martín, A. M. Harvey, and J. C. Braga, 134–185. Oxford: Blackwell. <https://doi.org/10.1002/9781444300604.ch6>.
- Martín Penela, J. A., Rodríguez Fernández, J., Barragán Bazán, G., Pascual, A., and Guerra Merchán, A. 1997. El registro sedimentario de las cuencas neógenas de la provincia de Almería. *Recursos Naturales y Medio Ambiente en el Sureste Peninsular* 1: 169–183.
- Martínez, J. M., and Azañón, J. M. 2002. Orthogonal Extension in the Hinterland of the Gibraltar Arc (Betics, SE Spain). *Journal of the Virtual Explorer* 8: 3–22.
- Martínez Martos, M., Galindo Zaldívar, J., and Martínez Moreno, F. J. 2017. Superposition of Tectonic Structures Leading Elongated Intramontane Basin: The Alhabia Basin (Internal Zones, Betic Cordillera). *International Journal of Earth Sciences* 106: 2461–71. <https://doi.org/10.1007/s00531-016-1442-9>.
- Masaitis, V., and Naumov, M. 2020. *The Puchezh-Katunki Impact Crater Geology and Origin: Geology and Origin. Impact Studies*. Springer, ebook. <https://doi.org/10.1007/978-3-030-32043-0>.
- Melosh, H. J. 1977. Crater Modification by Gravity: A Mechanical Analysis of Slumping. In *Impact and Explosion Cratering*, edited by D. J. Roddy, R. O. Pepin, and R. B. Merrill, 1245–60. New York, NY: Pergamon Press.
- Melosh, H. J. 1989. *Impact Cratering. A Geologic Process*. Oxford Monographs on Geology and Geophysics Series no. 11. ix + 245 Pp. Oxford: Clarendon Press. <https://doi.org/10.1017/S0016756800007068>.
- Ministerio de Transportes, Movilidad y Agenda Urbana. 2019. Plan Nacional de Ortografía Aérea (PNOA) <http://www.ign.es/iberpix2/visor/>.
- Ormö, J., Gómez-Ortiz, D., Mcguire, P. C., Henkel, H., Komatsu, G., and Rossi, A. P. 2007. Magnetometer Survey of the Proposed Sirente Meteorite Crater Field, Central Italy: Evidence for Uplifted Crater Rims and Buried Meteorites. *Meteoritic & Planetary Science* 42: 211–222. <https://doi.org/10.1111/j.1945-5100.2007.tb00228.x>.
- Ormö, J., Gulick, S. P. S., Whalen, M. T., King, D. T., Jr., Sturkell, E., and Morgan, J. 2021. Assessing Event Magnitude and Target Water Depth for Marine-Target Impacts: Ocean Resurge Deposits in the Chicxulub M0077A Drill Core Compared. *Earth and Planetary Science Letters* 564: 116915. <https://doi.org/10.1111/j.1945-5100.2008.tb00655.x>.
- Ormö, J., and Lindström, M. 2000. When a Cosmic Impact Strikes the Sea Bed. *Geological Magazine* 137: 67–80. <https://doi.org/10.1017/S0016756800003538>.
- Ormö, J., Nielsen, A. T., and Alwmark, C. 2017. The Vakkejokk Breccia: An Early Cambrian Proximal Impact Ejecta Layer in the North-Swedish Caledonides. *Meteoritic & Planetary Sciences* 52: 623–645. <https://doi.org/10.1111/maps.12816>.
- Ormö, J., Sturkell, E., Horton, J. W., Jr., Powars, D. S., and Edwards, L. E. 2009. Comparison of Clast Frequency and Size in the Exmore Sediment-Clast Breccia, Eyreville and Langley Cores, Chesapeake Bay Impact Structure: Clues to the Resurge Process. In *The ICDP-USGS Deep Drilling Project in the Chesapeake Bay Impact Structure: Results from the Eyreville Coreholes*, edited by G. S. Gohn, C. Koeberl, K. G. Miller, and W. U. Reimold. *Geological Society of America Special Paper*, 458, 617–32. Boulder, CO: Geological Society of America.
- Osinski, G. R., and Ferrière, L. 2016. Shatter Cones: (Mis) Understood? *Science Advances* 2: e1600616. <https://doi.org/10.1126/sciadv.1600616>.
- Osinski, G. R., Grieve, R. A. F., Ferrière, L., Losiak, A., Pickersgill, A. E., Cavosie, A. J., Hibbard, S. M., et al. 2022. A Review of the Terrestrial Impact Record. *Earth-Science Reviews* 232: 104112. <https://doi.org/10.1016/j.earscirev.2022.104112>.
- Osinski, G. R., Grieve, R. A. F., and Tornabane, L. L. 2013. Excavation and Impact Ejecta Emplacement. In *Impact Cratering: Processes and Products*, edited by G. R. Osinski, and E. Pierazzo, 43–59. West Sussex: Wiley-Blackwell Publishing. A John Wiley & Sons, Ltd., Publication. <https://doi.org/10.1002/9781118447307.ch4>.
- Osinski, G. R., and Pierazzo, E., eds. 2012. *Impact Cratering: Processes and Products*. Oxford: Wiley-Blackwell. <https://doi.org/10.1002/9781118447307>.
- Pedrera, A., Galindo Zaldívar, J., Marín-Lechado, C., García-Tortosa, F. J., Ruano, P., López-Garrido, A. C., Azañón, J. M., Peláez, J. A., and Gianola, F. 2012. Recent and Active Faults and Folds in the Central-Eastern Internal Zones of the Betic Cordillera. *Journal of Iberian Geology* 38: 191–208. https://doi.org/10.5209/rev_JIGE.2012.v38.n1.39213.
- Peucker-Ehrenbrink, B., and Bor-ming, J. 2001. Rhenium-Osmium Isotope Systematics and Platinum Group Element Concentrations: Loess and the Upper Continental Crust. *Geochemistry, Geophysics, Geosystems* 2. <https://doi.org/10.1029/2001GC000172>.
- Poag, W., Koeberl, C., and Reimold, W. U. 2004. *The Chesapeake Bay Crater: Geology and Geophysics of a Late Eocene Submarine Impact Structure; ESF IMPACT*. Berlin: Springer Science & Business Media, p. 522. [https://doi.org/10.1016/S0016-7878\(06\)80048-9](https://doi.org/10.1016/S0016-7878(06)80048-9).
- Poisson, A. M., Morel, J. L., Andrieux, J., Coulon, M., Wernli, R., and Guernet, C. 1999. The Origin and Development of Neogene Basins in the SE Betic Cordillera (SE Spain): A Case Study of the Tabernas-Sorbas and Huercaal-Overa Basins. *Journal of Petroleum Geology* 22: 97–114. <https://doi.org/10.1111/j.1747-5457.1999.tb00461.x>.
- Powars, D. S., and Bruce, S. 1999. The Effects of the Chesapeake Bay Impact Crater on the Geological

- Framework and Correlation of Hydrogeologic Units of the Lower York-James Peninsula, Virginia. U.S. Geological Survey Professional Paper 1612, USA Government Printing Office, Washington, DC, 91 pp. <https://doi.org/10.3133/pp1612>.
- Puga Bernabéu, A., Martín, J. M., and Braga, J. C. 2007. Tsunami-Related Deposits in Temperate Carbonate Ramps, Sorbas Basin, Southern Spain. *Sedimentary Geology* 199: 107–127. <https://doi.org/10.1016/j.sedgeo.2007.01.020>.
- Rudnick, R. L., and Gao, S. 2003. Composition of the Continental Crust. In *The Crust. Treatise in Geochemistry*, edited by R. L. Rudnick, vol. 3, 1–64. Amsterdam: Elsevier. <https://doi.org/10.1016/B978-0-08-095975-7.00301-6>.
- Sanz de Galdeano, C. 1985. Estructura del borde oriental de la Sierra de Gádor (zona Alpujárride, Cordilleras Béticas). *Acta Geológica Hispánica* 20: 145–154.
- Sanz de Galdeano, C., Shanov, S., Galindo Zaldívar, J., Radulov, A., and Nikolov, G. 2006. Neotectonics in the Tabernas Desert (Almería, Betic Cordillera, Spain). *Geosciences* 1: 75–78.
- Sanz de Galdeano, C., and Vera, J. A. 1991. Una propuesta de clasificación de las cuencas neógenas béticas. *Acta Geológica Hispánica* 26: 205–227.
- Sarv, K., Jöeleht, A., McCall, N., Gulick, S., Wilk, J., and Pösges, G. 2019. The Structure of Ries Crater Megablock Zone and Southern Rim Area According to Seismic Reflection Profiles. Large Meteorite Impacts VI (LPI Contribution no. 2136).
- Schmitz, B., Ellwood, B. B., Peucker-Ehrenbrink, B., El Hassani, A., and Bultynck, P. 2006. Platinum Group Elements and $^{187}\text{Os}/^{188}\text{Os}$ in a Purported Impact Ejecta Layer Near the Eifelian–Givetian Stage Boundary, Middle Devonian. *Earth and Planetary Science Letters* 249: 162–172. <https://doi.org/10.1016/j.epsl.2006.07.024>.
- Serrano, F. 1990. El Mioceno Medio en el área de Njar (Almería, España). *Revista de la Sociedad Geológica de España* 3: 65–77.
- Sola, F., Puga-Bernabéu, A., Aguirre, J., and Braga, J. C. 2018. Origin, Evolution and Sedimentary Processes Associated with a Late Miocene Submarine Landslide, Southeast Spain. *Sedimentary Geology* 364: 351–366. <https://doi.org/10.1016/j.sedgeo.2017.09.005>.
- Stöffler, D., and Langenhorst, F. 1994. Shock Metamorphism of Quartz in Nature and Experiment: I Basic Observation and Theory. *Meteoritics* 29: 155–181. <https://doi.org/10.1111/j.1945-5100.1994.tb00670.x>.
- Sturkell, E. 1998. Impact-Related Ir Anomaly in the Middle Ordovician Lockne Impact Structure, Jämtland, Sweden. *GFF* 129: 333–336. <https://doi.org/10.1080/11035899801204333>.
- Tagle, R., Erzinger, J., Hecht, L., Schmitt, R. T., Stöffler, D., and Claeys, P. 2004. Platinum Group Elements in Impactites of the ICDP Chicxulub Drill Core Yaxcopoil-1: Are there Traces of the Projectile? *Meteoritics & Planetary Science* 39: 1009–16. <https://doi.org/10.1111/j.1945-5100.2004.tb00942.x>.
- Taylor, S. R., and McLennan, S. M. 1985. *The Continental Crust: Its Composition and Evolution*. Oxford: Blackwell Scientific Publications. 312.
- Taylor, S. R., and McLennan, S. M. 1995. The Geochemical Evolution of the Continental Crust. *Geophysics* 33: 241–265. <https://doi.org/10.1029/95RG00262>.
- Velando, F., Navarro, D., and de las Heras, A. 1979. Hoja 1029 (Gérgal) del Mapa Geológico de España E. 1:50.000. Mapa y memoria. IGME.
- Voermans, F., Baena, J., Ewert, K., Granados Granados, L. F., Martínez Díaz, C., Fernández, M. C., and Argüelles, A. 1983. Hoja 1044 (Alhama de Almería) del Mapa Geológico de España E. 1:50.000. Mapa y memoria. IGME.
- Voermans, F., Baena, J., Martínez, C., Granados, L. F., Fernández, M. C., Argüelles, A., del Pan, T., and Mansilla, H. 1983. Hoja 1045 (Almería) del Mapa Geológico de España E. 1:50.000. Mapa y memoria. IGME.
- Weijermars, R. 1991. Geology and Tectonics of the Betic Zone, SE Spain. *Earth-Science Reviews* 31: 153–236. [https://doi.org/10.1016/0012-8252\(91\)90019-C](https://doi.org/10.1016/0012-8252(91)90019-C).
- Weijermars, R., Roep, T. B., Van den Eeckhout, B., Postma, G., and Kleverlaan, K. 1985. Uplift History of a Betic Fold Nappe Inferred from Neogene-Quaternary Sedimentation and Tectonics (in the Sierra Alhamilla and Almería, Sorbas and Tabernas Basins of the Betic Cordilleras, SE Spain). *Geologie en Mijnbouw* 64: 397–411.
- Wünnemann, K., Morgan, J. V., and Jödicke, H. 2005. Is Ries Crater Typical for its Size? An Analysis Based upon Old and New Geophysical Data and Numerical Modeling. In *Large Meteorite Impacts III*. GSA Special Paper 384, edited by T. Kenkmann, F. Hörz, and A. Deutsch, 67–83. Boulder, CO: Geological Society of America. <https://doi.org/10.1130/0-8137-2384-1.67>.

SUPPORTING INFORMATION

Additional supporting information may be found in the online version of this article.

Data S1.